Design and Realization of an FMCW/Doppler Radar

By Naveed Edalati, Rohan Phadke, Charles Paulekas, and Ruchika Jingar

Abstract

From the turn of the 20th century Radars have played a pivotal role in the progression of human society. Military applications proved to be the primal impetus behind the advancements in Radar technologies. In World War II these systems revolutionized reconnaissance capabilities and aided the allied powers in their triumphs and eventual victory. As the war came to an end these systems began to be associated with a plethora of new and innovative applications. These applications include remote sensing, air traffic control, law enforcement and security, space, air safety, navigation, medical imaging, weather forecasting, and radar interferometry. Nevertheless, the basic concepts and building blocks of all radar systems are very similar. Through outlining the design, manufacturing, and testing process for a simple FMCW and Doppler radar our group aims to present a radar design that can be utilized for several applications and across many disciplines.

Introduction

The primary purpose of this paper is to present the design and implementation of a comprehensive system that acts as both a Frequency Modulated Continuous Waveform (FMCW) and Doppler radar. The dual capabilities that this radar can support make it widely applicable for use in an extensive range of radar applications. FMCW radars can be used to locate and detect objects, while Doppler radars can help to determine the speed of an object. Nevertheless, the most important design consideration was the complexity of the system. Modern radars can be extremely complex systems to design and analyze. Added features such as advanced signal processing techniques have expanded the capabilities of radars immensely. Additionally, advancements in radio frequency integrated circuits have allowed for single chip transceivers. Nevertheless, these added complexities often overlook the basic and integral building blocks of radars. The main goal of this project was to design a simple radar system that could be easily built and used in a wide range of applications. In order to accomplish this, the design emphasis was put on the basic and traditional building blocks of a radar system. These basic building blocks pertain to three distinct categories. The first is the overall RF System design, the second is the baseband signal processing, and the third is the antenna design. The RF system design consists of the high frequency devices that go into the Transmit and Receive portions of the radar. These devices may serve to generate high frequency signals, provide amplification to signals, alter the frequency of signals, direct signals through particular paths, or attenuate signals. The signal being generated and received by the RF System must eventually be mixed to a lower frequency in order for the information to be digitally processed. When mixed the signal can be and in most instances must be altered. Therefore, baseband signal processing is used to accomplish this. Specifically, the devices that fall under the baseband signal-processing category can amplify a signal and can allow for filtering capabilities. In addition to the RF and baseband devices another imperative building block of radars are the antennas. Antennas are the devices that allow for the electrical signals within the system to be transferred through the air as electromagnetic signals and later be received. Additionally, antennas themselves can provide amplification. This paper will fully examine the details of each one of the aforementioned categories. Nevertheless, the first task will be to outline the overall system specifications of the radar being designed. Secondly, the design and implementation of the RF subsystem, baseband subsystem, and the antenna will be thoroughly examined. Lastly, a comprehensive discussion of the testing and performance of the overall system will be carried out.

Overall System Specifications

The system specifications for this radar were constrained by the ISM (Industry, Scientific and Medical) radio band. Thus, it was chosen that the radar would operate within the 2.4GHz band. The total transmit power was dependent on the range of the radar. The system was designed to receive approximately -70dbm at 20 meters. Using Frii's equation, the required transmit power, when considering a .3 square meter target, was determined to be approximately 15dbm. In summary, the system was chosen to operate at 2.4 GHz with an output power level of approximately 15dbm. Since the FMCW radar design requires modulation, a frequency range had to be chosen in addition to the operational frequency. The frequency range was chosen to be 2.3-2.6GHz.

Design and Implementation

This section will discuss the design and implementation of the RF subsystem, baseband subsystem, and the antennas utilized in this system. The block diagram of the RF subsystem and the selection of the individual components will be outlined. Then the amplifier and filter design utilized in the baseband subsystem will be presented. Next, the design of the antenna will be thoroughly examined. Finally, the implementation of the respective subsystems and antennas will be explored.

RF Subsystem

The RF subsystem consists of a three primary paths. These include the Transmit, the Local Oscillator, and the Receive paths. The Transmit path begins with a simple modulating circuit that drives the tuning voltage of a modular VCO. The VCO is followed by a modular LNA that provides substantial amplification to the RF signal. There is a Power splitter that follows the modular LNA. The first Port of the power splitter directs the RF power to the transmit antenna. The second port of the splitter leads to the Local Oscillator path. The LO path begins with a 3dB attenuator placed after the second port of the splitter. This attenuator comes before the LO port of a passive mixer, which typically exhibit poor matching characteristics. The attenuator acts to reduce the amount of reflected power back towards the RF path. The Local oscillator path then feeds to the LO port of the Mixer. The receive path consists of a patch antenna that directs the incoming signals to a cascade of modular LNAs. The series of LNAs apply substantial gain to the signals that are received by the system. Finally, the RF path feeds to the RF port of the mixer, which is used to mix the incoming signal so that it may be analyzed and interpreted. The full system diagram can be examined on the next page. In addition to illustrating the system layout, the power levels and pertinent device parameters are outlined in the Block Diagram. It's important to note that the specifications outlined in the block diagram vary within the operating frequency range (2.3-2.6GHz).

RF Subsystem Block Diagram

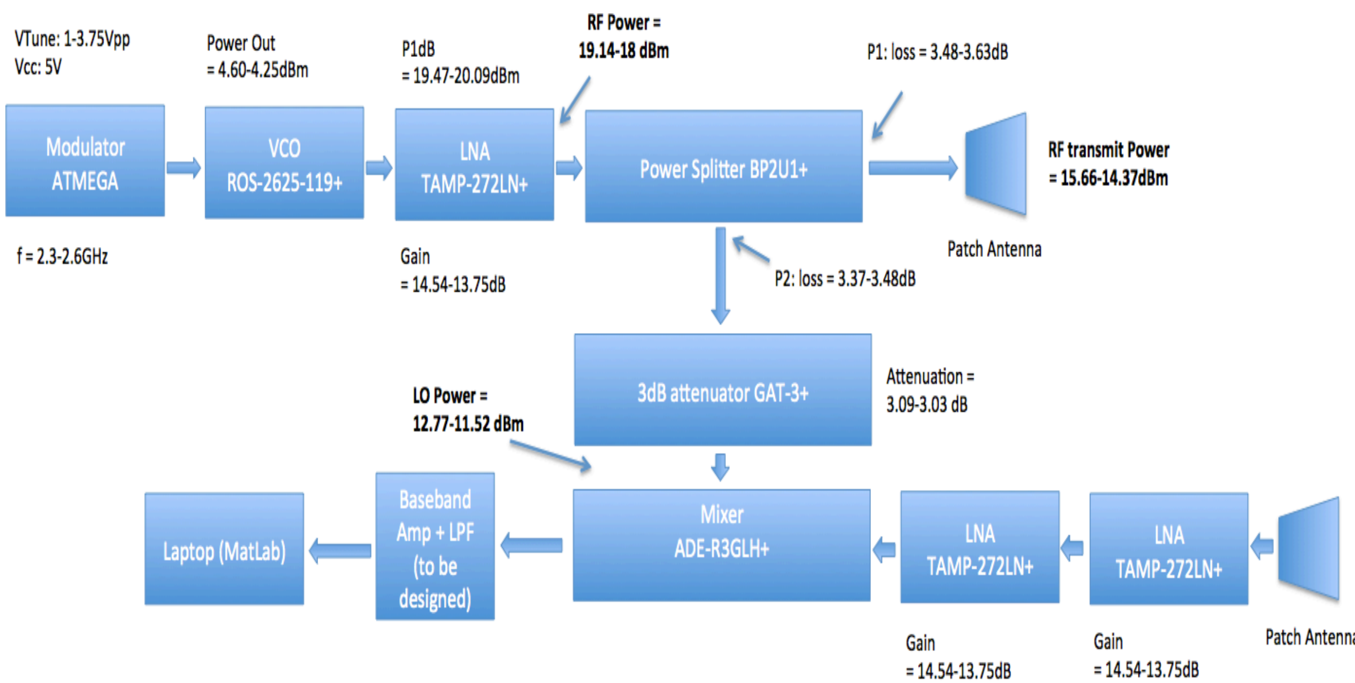

The devices that were chosen for each element in the RF subsystem can be seen and analyzed in the table on the next page

RF Subsystem Device Summary

Device	Manufacturer	Model	Specification
Voltage controlled Oscillator (VCO)	Mini Circuits	ROS-2625-199+	Power Output: +4dBm
Low Noise Amplifiers (LNAs)	Mini Circuits	TAMP-272LN+	Gain: 14.5dB Gain Flatness: +/- .5dB Noise Figure: .85dB
Power Splitter	Mini Circuits	BP2U1+	Insertion Loss: 3.5 dB
Fixed Attenuator	Mini Circuits	GAT-3+	Attenuation: 3dB
Mixer	Mini Circuits	ADE-R3GLH+	LO Power + 10 dBm Conversion loss: 5.2dB LO-RF isolation: 5.2dB

In addition to the Block diagram and device summary outlined above, a link budget for the Transmit and Local oscillator paths was completed separately and can be examined below.

Summary of Link Budget Analysis for LO and Transmit paths

Frequency	Local Oscillator Power	RF transmit Power
2.3 GHz	$\mathbf{12.77 dBm}$	$\mathbf{11.52 dBm}$
2.6 GHz	$\mathbf{15.66 dBm}$	$\mathbf{14.27 dBm}$

$$\boldsymbol{LO\ Power\ Swing = 12.77dBm - 11.52dBm}$$

$$\boldsymbol{RF\ transmit\ Power\ Swing = 15.66dBm - 14.27dBm}$$

A comprehensive link budget was completed for the entire system. This particular calculation considered what the received power level would be based off the transmit power. Additionally the calculations were made for a .3 square meter object placed at a variety of distances. The following tables summarize the aforementioned link budget.

Received Power vs. Range

Range	Power Received
1m	-21.58dBm
10m	-65.53dBm
25m	-81.44dBm
50m	-93.28dBm

Finalized Link Budget (Receive Power)

Range	Power Received	Mixer Output Power	Mixer Output Voltage
1m	-21.58dBm	-3.53dBm	420.74mVpp
10m	-65.53dBm	-43.53dBm	4.21mVpp
25m	-81.44dBm	-59.44dBm	673.78uVpp
50m	-93.28dBm	-71.48dBm	168.47uVpp

The amount of current that the RF subsystem is drawing is a very important factor to consider. Specifically, when designing a PCB the total current being drawn from the power supply must be known, in order to utilize a proper track width for the supply rail.

RF Subsystem Current Draw

Component	Current Draw
LNA (x3)	60 mA
VCO	35 mA
ATMEGA processor (Modulator circuit)	4 mA
DAC (Modulator circuit)	250 uA

$$\boldsymbol{Total\ DC\ current = 219.25mA}$$

Baseband Subsystem

The baseband subsystem primarily consists of the gain stage required to boost the amplitude of the output of the mixer, a filter stage to filter unwanted frequencies and then an audio jack output to connect to the computer. The gain stage consists of two noninverting op amps in cascade. The gain stage is optimized for an input signal of amplitude 100 mVpp and so will provide a gain of 10 to give a signal with amplitude 1 Vpp. The filter is a dedicated IC and the filter itself is an 8^{th} order Butterworth filter. The cutoff frequency of the filter is set to 12 kHz through an external 22 pF capacitor and the filter provides no gain to the system. The audio jack output goes to the computer where the IF signal is sampled at a rate of 44.1 kHz. Then MATLAB code is used to process the IF signal to get the desired output.

Baseband Subsystem Block Diagram

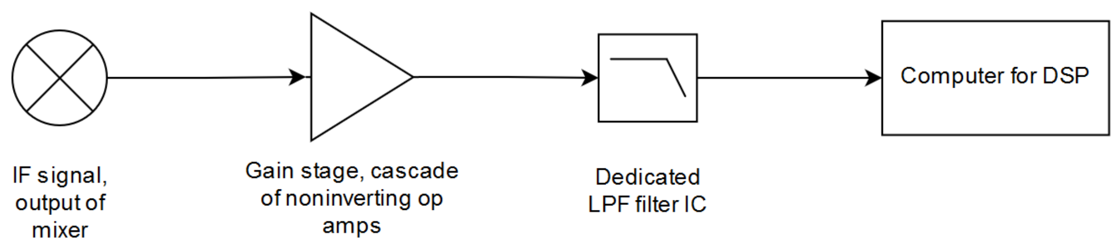

The ICs that were chosen for each element in the baseband subsystem are shown in the table below.

Baseband Subsystem Device Summary

Device	Manufacturer	Model
Operational Amplifier (Op Amp)	Texas Instruments	TI OPA2227
Low Pass Filter (LPF)	Maxim Integrated	MAX291CSA+-ND

The table below outlines the expected current draw of the ICs mentioned above.

Baseband Subsystem Current Draw

Component	Current Draw
Op amp	7.4 mA
LPF	15 mA

$$\boldsymbol{Total\ DC\ current = 22.4\ mA}$$

In addition to the block diagram and the device summary outlined above two tables containing the IF frequency for both tests in the competition are shown below. These tables helped in the determination of the cutoff frequency.

IF Frequencies for Test 1

Range R	IF frequency
5 m	0.5 kHz
50 m	5 kHz

IF frequencies for Test 2

Frequency	Amplitude	IF frequency
0.2 Hz	1 mm	0.0201 Hz
	10 mm	0.2011 Hz
0.8 Hz	1 mm	0.0804 Hz
	10 mm	0.8042 Hz

The screenshot below is a TINA-TI SPICE simulation of the gain stage. This simulation confirms that the gain stage design is working properly since the amplitude of the signal is 1 Vpp. The TINA schematic and simulation output is shown below.

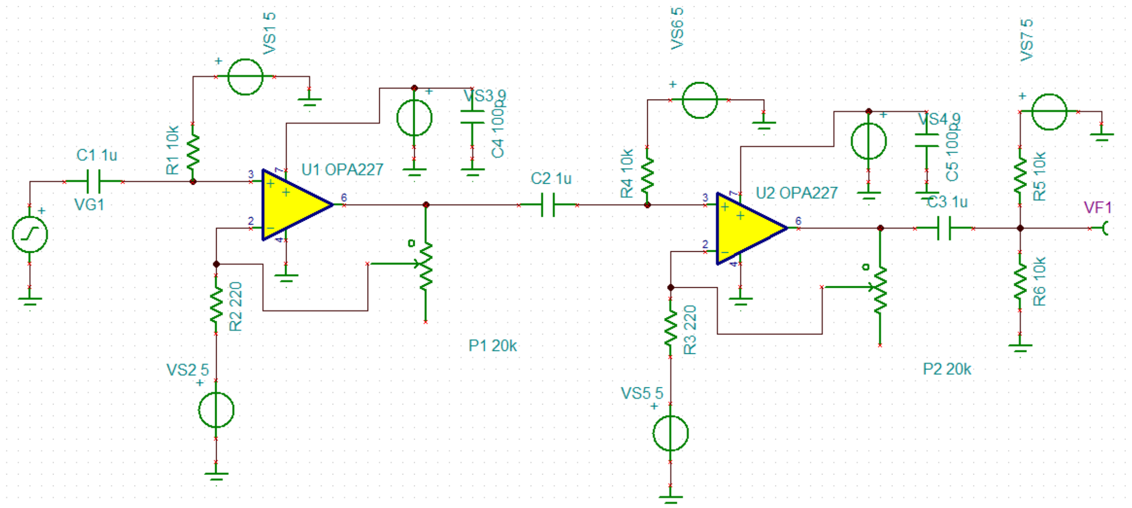

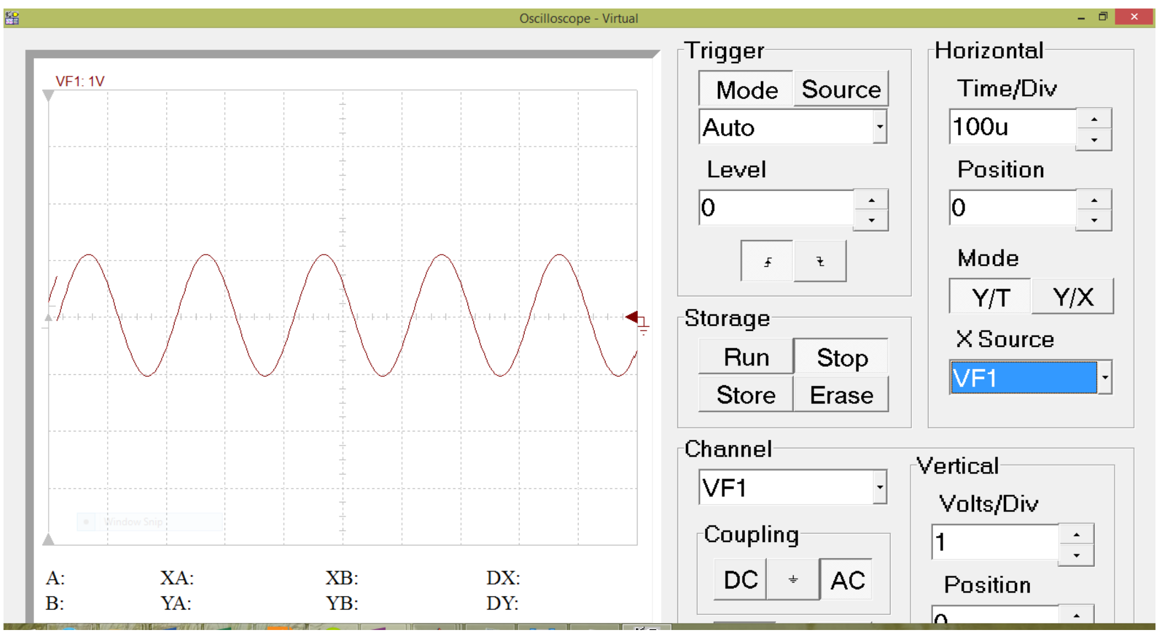

The MATLAB code below is used to process the .wav file recorded for the radar range measurement.

```
%MIT IAP Radar Course 20112.5
%Resource: Build a Small Radar System Capable of Sensing Range,
Doppler,
```

```
%and Synthetic Aperture Radar Imaging
%
%Gregory L. Charvat

%Process Range vs. Time Intensity (RTI) plot

clear all;
close all;

% read the raw data .wav file here
% replace with your own .wav file
[Y,FS,NBITS] = wavread('radar_range.wav');

%constants
c = 3E8; %(m/s) speed of light

%radar parameters
Tp = 20E-3; %(s) pulse time
N = Tp*FS; %# of samples per pulse
fstart = 2260E6; %(Hz) LFM start frequency
fstop = 2590E6; %(Hz) LFM stop frequency
BW = fstop-fstart; %(Hz) transmti bandwidth
f = linspace(fstart, fstop, N/2); %instantaneous transmit frequency

%range resolution
rr = c/(2*BW);
max_range = rr*N/2;

%the input appears to be inverted
trig = -1*Y(:,1);
s = -1*Y(:,2);
clear Y;

%parse the data here by triggering off rising edge of sync pulse
count = 0;
thresh = 0;
start = (trig > thresh);
for ii = 100:(size(start,1)-N)
    if start(ii) == 1 & mean(start(ii-11:ii-1)) == 0
        %start2(ii) = 1;
        count = count + 1;
        sif(count,:) = s(ii:ii+N-1);
        time(count) = ii*1/FS;
    end
end
%check to see if triggering works
% plot(trig,'.b');
% hold on;si
% plot(start2,'.r');
% hold off;
% grid on;

%subtract the average
ave = mean(sif,1);
for ii = 1:size(sif,1);
    sif(ii,:) = sif(ii,:) - ave;
end
```

```
zpad = 8*N/2;

%RTI plot
figure(10);
v = dbv(ifft(sif,zpad,2));
S = v(:,1:size(v,2)/2);
m = max(max(v));
imagesc(linspace(0,max_range,zpad),time,S-m,[-80, 0]);
colorbar;
ylabel('time (s)');
xlabel('range (m)');
title('RTI without clutter rejection');

%2 pulse cancelor RTI plot
figure(20);
sif2 = sif(2:size(sif,1),:)-sif(1:size(sif,1)-1,:);
v = ifft(sif2,zpad,2);
S=v;
R = linspace(0,max_range,zpad);
for ii = 1:size(S,1)
    %S(ii,:) = S(ii,:).*R.^(3/2); %Optional: magnitude scale to
range
end
S = dbv(S(:,1:size(v,2)/2));
m = max(max(S));
imagesc(R,time,S-m,[-80, 0]);
colorbar;
ylabel('time (s)');
xlabel('range (m)');
title('RTI with 2-pulse cancelor clutter rejection');
```

The code above reads a stored .wav file and converts the data into the frequency domain using the Fast Fourier Transform (FFT). Then the maximum amplitude of the data is found, both before and after performing clutter rejection.

The MATLAB code shown below is realtime code used for the Doppler test.

```
%This code originated from sample code given by Gregory Charvat.
It's been heavily 'developed' into the code
%that you see now primarily by Zach Myers. However intermediate
versions were developed by Jhonnaton Ascate
% and Christopher Young.
clear all;
close all;

%constants
dbv = @(x) 20*log10(abs(x));
c=3E8; %(m/s) speed of light

%radar parameters
FS = 44.1E3;
Tp = 0.1; %(s) pulse time
N = 8000; %# of samples per pulse
fc = 2590E6; %(Hz) Center frequency (connected VCO Vtune to +5)
```

```
recordLength = 0.20;

%filters:
%K: Used to filter incoming signal
%K = Test23;
%K3: Used to window receive signal to reduce sidelobe noise
K3 = hanning(100);


%Recording Setup
r = audiorecorder(44100,16,2);
record(r);
pause(recordLength);
stop(r)
Y= getaudiodata(r);

%Set up shift register buffer
bufferVel = [];
bufferSize = 30;
bufferPosition = 0;

%All of the plots are initialized ahead of time and the set function
is used
%later on instead of recalling plot

%Calling plot continuously is inefficient because it reinitializes
memory whereas
%set simply changes one or two arrays

%Output of Dopplar Radar AFTER windowing
figure(1);
H = plot(Y);
H1 = axis;
ylabel('Amplitude of Doppler Shift (volts)');
xlabel('Time (sec)');
title('Doppler Radar - Received Signal (After Filtering)');
ylim([-5 5]);
xlim([0.005 0.08]);
C = 1;

%Waterfall-ish Diagram
figure(2);
H2 = mesh([0 1;2 3]);
ylim([1 Tp*bufferSize]);
xlim([0 50]);
zlim([-140 10]);
xlabel('Velocity (m/sec)');
ylabel('Time (sec)');
title('Doppler Radar - Velocity');

%Incredibly Rough Peak Detection Algorithm Display
figure(3);
H3 = plot(0,0);
title('Shift Buffer of Maximum Readings over -40 dB');
xlabel('Position in Buffer');
ylabel('Approximate Velocity (m/s)');
```

```
highspeed = zeros(bufferSize,1);
while 1,
    %While everything is processing, have the audio recorder record
audio - This is basically a ping pong buffer - one buffer is
processed
    %as another buffer is filled - although MATLAB obsfucates what
buffer is being filled with the recorder wrapper class
    record(r);

    %the input appears to be inverted <- MIT comment
    s = -1*Y(:,2);

    %The signal is windowed by a hanning filter
    K3 = hanning(length(s));
    s = s.*K3;
    %s= filter(K, s);

    %This displays the windowed data to one graph
    set(H, 'YData', s(3:end), 'XData', (3:1:size(s,1))/FS);

    %create doppler vs. time plot data set here
    sif(1,:) = s(1:N);

    %subtract the average DC term here
    sif = sif - mean(s);
    zpad = 8*N/2;

    %doppler vs. time plot:
    %This takes the fourier transform of the signal - I am not sure
why MIT chose to use the IFFT over the FFT
    v = dbv(ifft(sif,zpad,2));
    v = v(:,1:size(v,2)/2);

    %This section attempts to do a very rudimentary form of peak
detection based on the top 3 highest signals
    A = sort(v(3:end), 'descend');
    %The three dopplar shifts that have the largest reflection are
averaged together - this might require significant tweaking
    %as there is significant near-DC components that need to be
accounted for
    B(1) = find(v == A(1));
    B(2) = find(v == A(2));
    B(3) = find(v == A(3));
    A2 = mean(A(1:3));

    %This whole section could be optomized by manually tracking
increase in
    %size - however it was not necessary due to the large amount of
    %processing power

    %In fact, this loop does not occupy enough time so I had to
insert a delay later inorder for the number of samples accumulated
to be appropiate.
    bufferVel = [bufferVel; v];
    if size(bufferVel,1) > bufferSize;
        bufferVel = bufferVel((size(bufferVel,1)- bufferSize +
1):end,:);
```

```
    end

    %calculate velocity
    delta_f = linspace(0, FS/2, size(bufferVel,2)); %(Hz)
    lambda=c/fc;
    velocity = delta_f*lambda/2;
    avePeakVelo = (velocity(B(1))*A(1) + velocity(B(2))*A(2) +
velocity(B(3))*A(3))/(sum(A(1:3)));

    %calculate time
    time = linspace(1,Tp*size(bufferVel,1),size(bufferVel,1));
%(sec)

    %plot
    set(H2, 'XDATA',velocity(3:700), 'YDATA', time(1:end), 'ZDATA',
bufferVel(1:end,3:700));
    if A2 > -52,%this determines what is considered a detection - it
is set manually (which is bad due to environment dependencies).
        highspeed = [highspeed; avePeakVelo];
        if size(highspeed,1) > bufferSize;
            highspeed = highspeed((size(highspeed,1)- bufferSize +
1):end,:);
        end
        set(H3, 'XDATA', 1:1:bufferSize, 'YDATA', highspeed);
    end

    clear SS S v sif ave count start thresh s trig time velocity;
    %Here is where the delay comes into play - after all the
processing is done
    pause(recordLength);
    %Stop recording and saving the audio data into Y
    stop(r);
    Y = getaudiodata(r);
end
```

This code processes the real time data using the concept of a shift buffer. Essentially what it does is that it first windows the incoming signal and displays this windowed data. It then stores a certain amount of values into a buffer vector. Then, the FFT of the data is taken, the velocity is calculated and the maximum velocity is found using a rudimentary form of peak detection. All this data is then plotted. After plotting, the values are updated by "pushing" out the old values and "pushing" in the next set of values.

<u>Wideband E-Shaped Patch Antenna</u>

As was discussed in the specifications section above, our purpose was to design a low profile, lightweight antenna for use at 2.4 GHz over a certain frequency band. From our calculations we found that in order to capture the frequency range for the Doppler test we would need a 10% bandwidth about 2.4 GHz. Due to the nature of the standard rectangular patch antenna, the patch responds fairly well at a single frequency, with its S_{11} parameter dropping well below -30 dB. However, because our application required a larger frequency range a more sophisticated patch antenna had to be designed. In order to fulfill the requirements of the system we turned to a research paper regarding wideband patch antennas by Ang and Chung titled *A Wideband E-Shaped Microstrip Patch Antenna For 5-6 GHz Wireless Communications*.

The paper by Ang and Chung described an experimental design that involves cutting two parallel slots in a probe-fed patch antenna along one side and removing a small patch in between them:

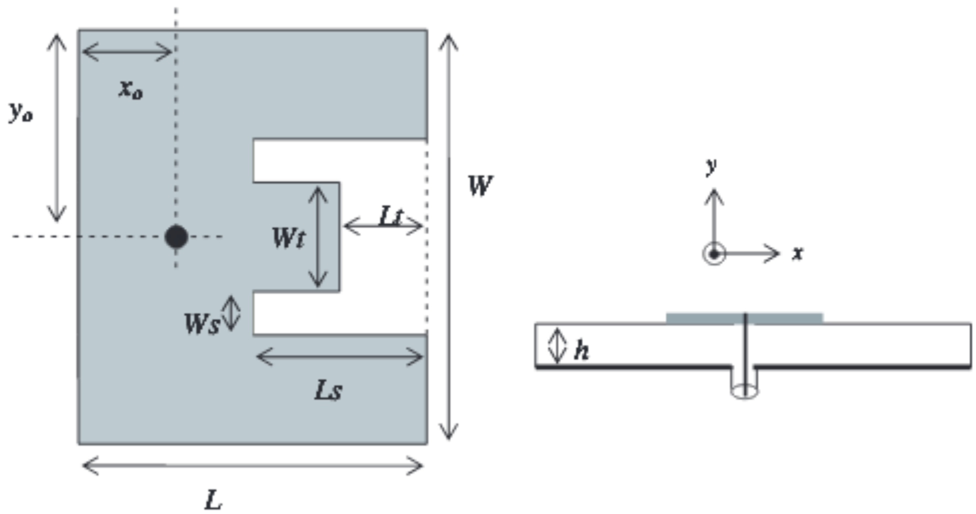

The idea behind this design is to create two resonant points within the patch structure both along the middle section of the E and along the two outer arms whose position in the frequency domain can be modified by changing the dimensions of Lt, Wt, Ws, and Ls given in the above figure. It was found experimentally that increasing the values of Ws, Ls, and Wt would decrease the location of one of the resonant point by increasing the distance traveled to reach the end of the arm, which would produce an increasing inductive effect. It was similarly found that decreasing Lt and increasing Wt to make the center section larger would have a comparable effect on the second resonant points, making its response appear at a lower frequency.

The patch design in the original paper was intended for use at a resonance of 5.25 GHz with a frequency range of 5.15 – 5.825 GHz. We began with choosing a suitable PCB substrate. We found that Rogers produces a substrate designed specifically for microstrip antennas designated RO4725JXR, which has a dielectric constant of 2.65 with the option of a 1.542 mm dielectric thickness and 35 μm copper cladding. With these parameters in hand we employed the equations for a standard rectangular patch antenna:

$$W = \frac{V_o}{2f_r}\sqrt{\frac{2}{\varepsilon_r + 1}}$$

$$\varepsilon_{\mathrm{reff}} = \frac{(\varepsilon_{\mathrm{r}} + 1)}{2} + \frac{(\varepsilon_{\mathrm{r}} - 1)}{2}\left[1 + \frac{12h}{w}\right]^{-\frac{1}{2}}$$

$$\frac{\Delta \mathrm{L}}{\mathrm{h}} = \frac{0.412\left((\varepsilon_{\mathrm{reff}} + 0.3)\left(\frac{W}{\mathrm{h}} + 0.264\right)\right)}{(\varepsilon_{\mathrm{reff}} - 0.258)\left(\frac{W}{\mathrm{h}} + 0.8\right)}$$

$$L = \frac{v_o}{2f_r\sqrt{\varepsilon_{\mathrm{reff}}}} - 2\Delta \mathrm{L}$$

Employing these equations resulted in our prototype patch size with a width of 46.32808 mm and length of 37.86729 mm.

With the standard patch in hand we then had to cut the slots in order to achieve the frequency response we desired. We performed some simple scaling from the dimensions given in the paper by Ang and Chung in order to get dimensions that would give us a response in the ballpark of what we originally intended. From here we performed a parametric analysis of each of the other dimensions of yo, xo, Wt, Lt, Ls, and Ws as was done in the paper in order to arrive at a frequency response we desired.

PCB Implementation

The entire system, except for the antennas, was implemented as a PCB. There are several factors that must be considered when designing high frequency PCB's. The PCB was designed so that the entire system would be combined into a signal two-layer board. Nevertheless, the RF and baseband subsystems were adequately separated to insure proper isolation and reduce the effects of interference. The program utilized to complete the PCB design was KiCad. The PCB schematic for the entire system can be seen below.

PCB Schematic

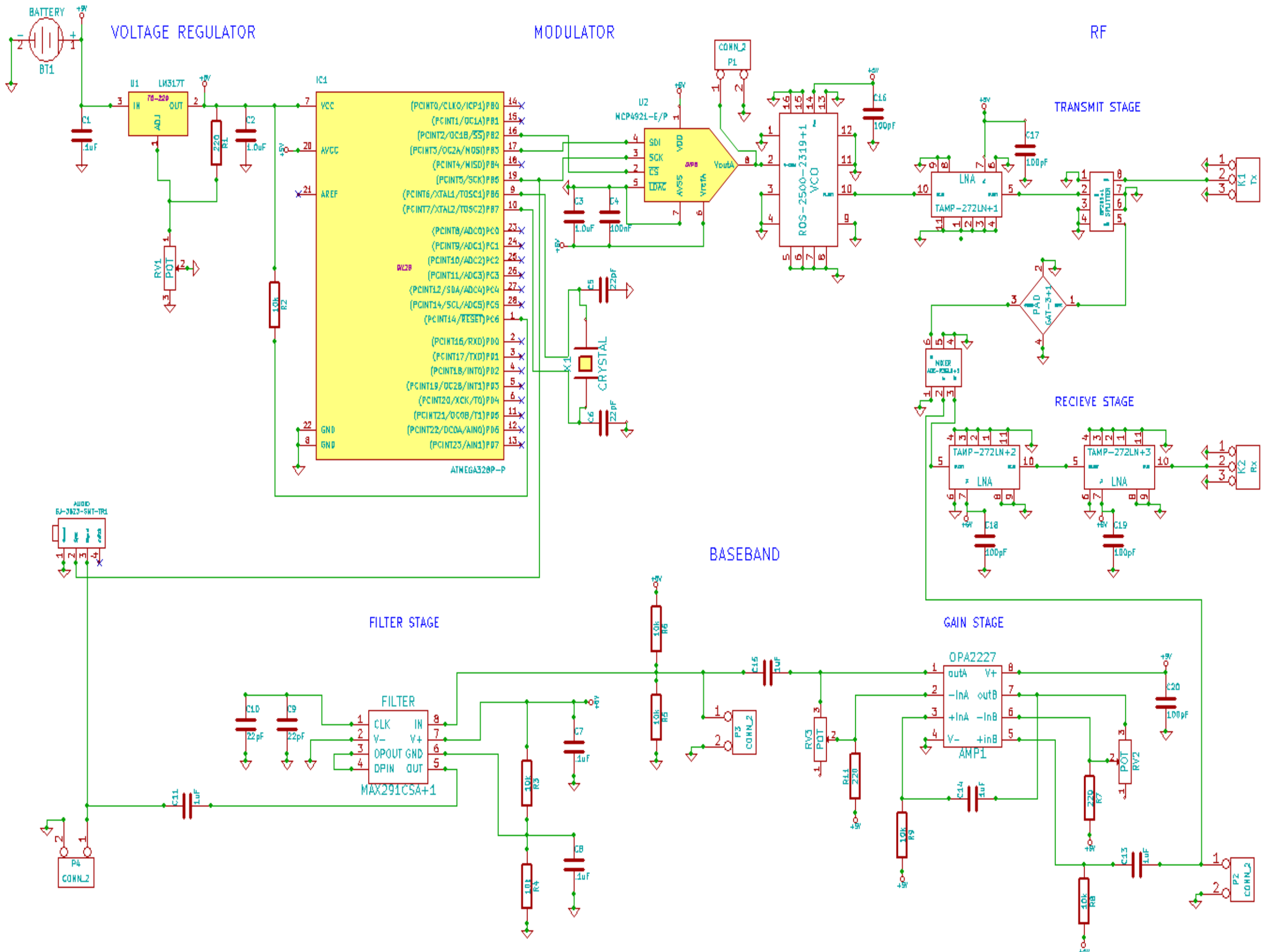

Once the schematic for the entire system was put together, each individual component was assigned to its corresponding footprint using CvPCB in Kicad.

CvPCB for the Overall System

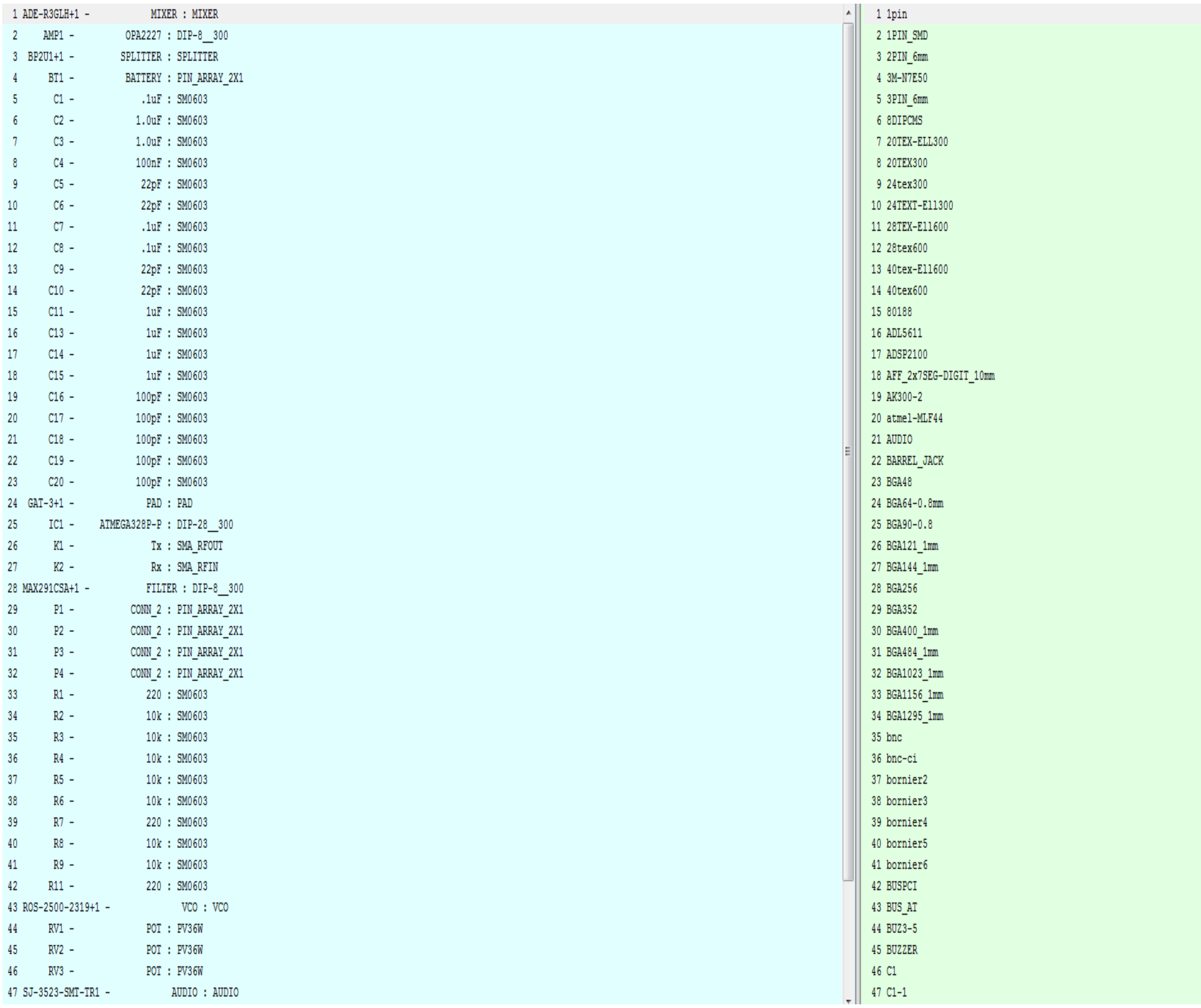

The final step in the implementation of the RF and baseband subsystems was to complete the PCB layout. In addition to laying out the board so that the Baseband and RF portions were isolated, there were two important calculations that had to be completed. Firstly, the trace width of the power rail had to be determined based off of the current draw of the entire system. It was previously determined that the current draw of the entire system was approximately 219.25mA. Using the PCB calculator on the Advanced Circuits webpage the required trace width was determined to be approximately 2.00 mil.

The second PCB parameter that had to be determined was the width and separation of a coplanar waveguide that would be used to provide 50 ohm matching between the RF components. The following diagrams outline the calculations that were completed for the dimensions of the coplanar waveguide.

Grounded Coplanar Waveguide Calculations

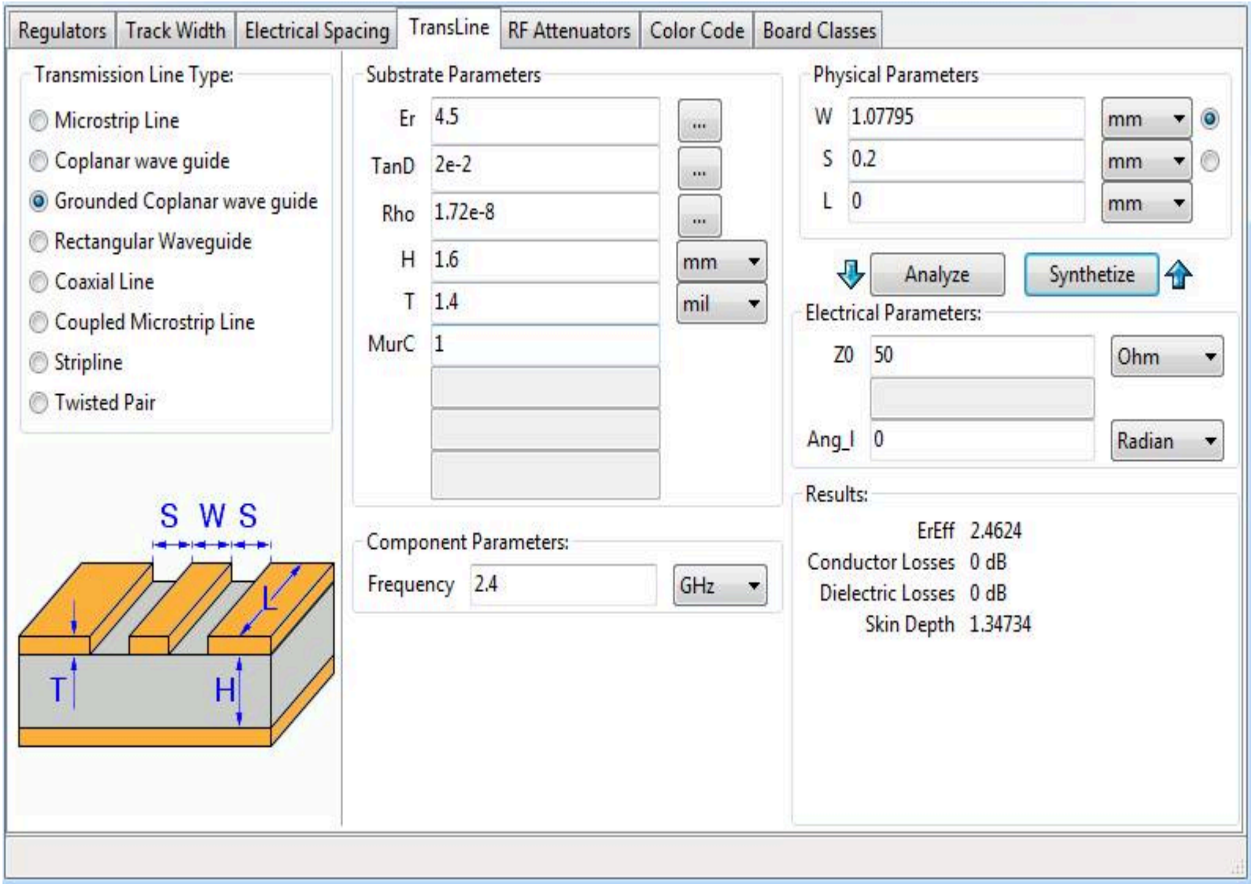

The critical PCB parameters are summarized in the Table below.

RF Subsystem PCB Summary

Number of Layers	Substrate Parameters	Required Power Rail Width	Coplanar Waveguide Specifications
2-layers	Er: 4.5 (FR4) H: 1.6 mm T: 1.4mil	W: 2 mil	Width: 1.07795 mm Separation: 0.2 mm

Confirmation of Coplanar Waveguide Calculations in ADS

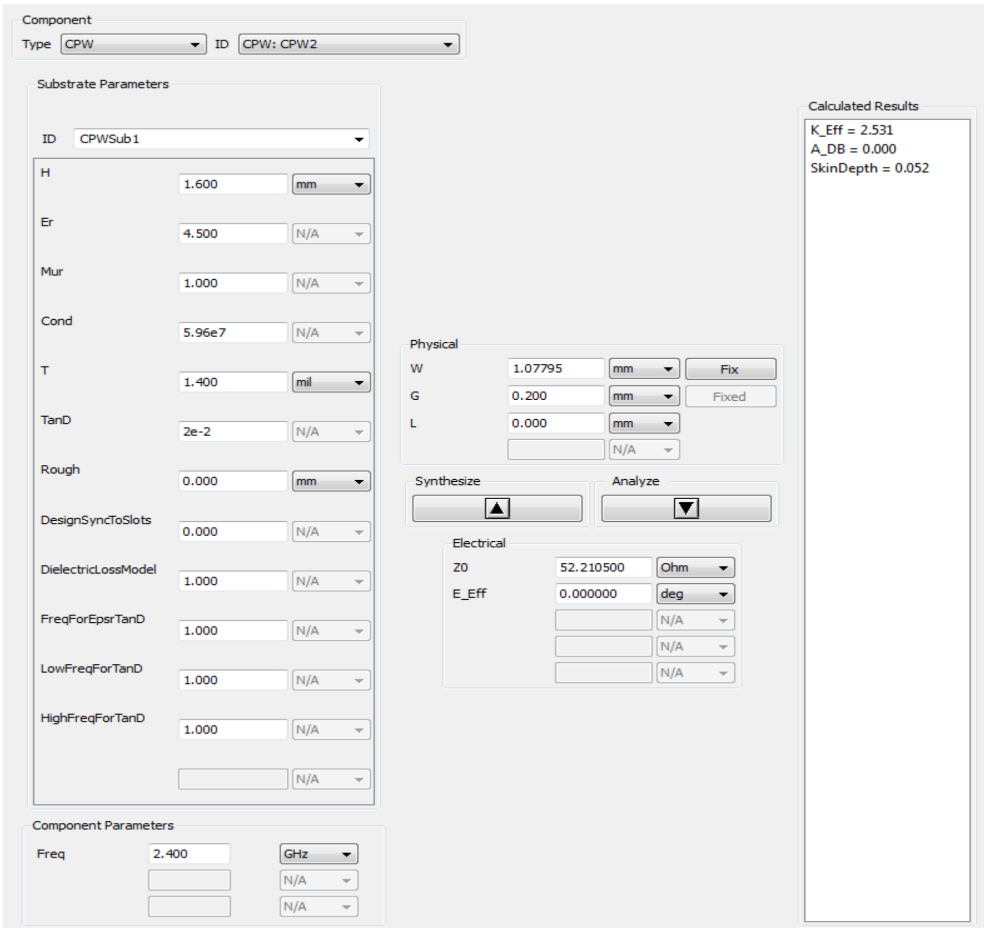

With the physical characteristics of the PCB layout determined, the actual design of the layout was completed. In order to implement the coplanar waveguide the top and bottom layers had to be designated as ground planes. The vias that were utilized helped to stitch these designated ground planes together. The final PCB layout can be examined on the next page.

Final PCB Layout

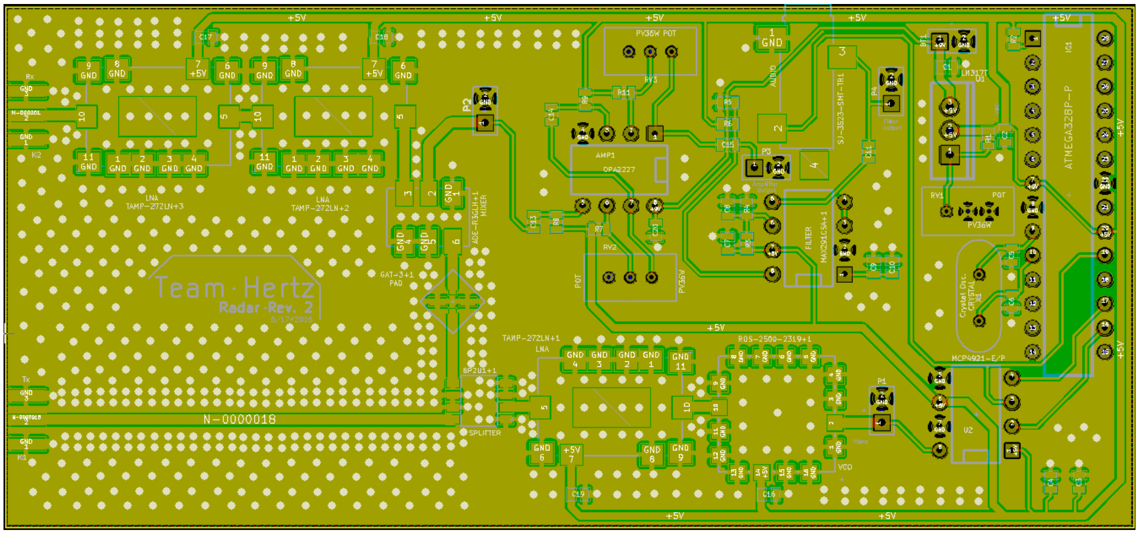

The RF portion of the layout begins at the bottom center of the board and continues onto the left side, while the baseband circuit is concentrated on the right side. The thickest traces in the layout resemble the coplanar waveguides. The distances between each RF component were kept small to reduce the effects of mismatches. A three dimensional view of the layout is provided below.

3D view of Final PCB Layout

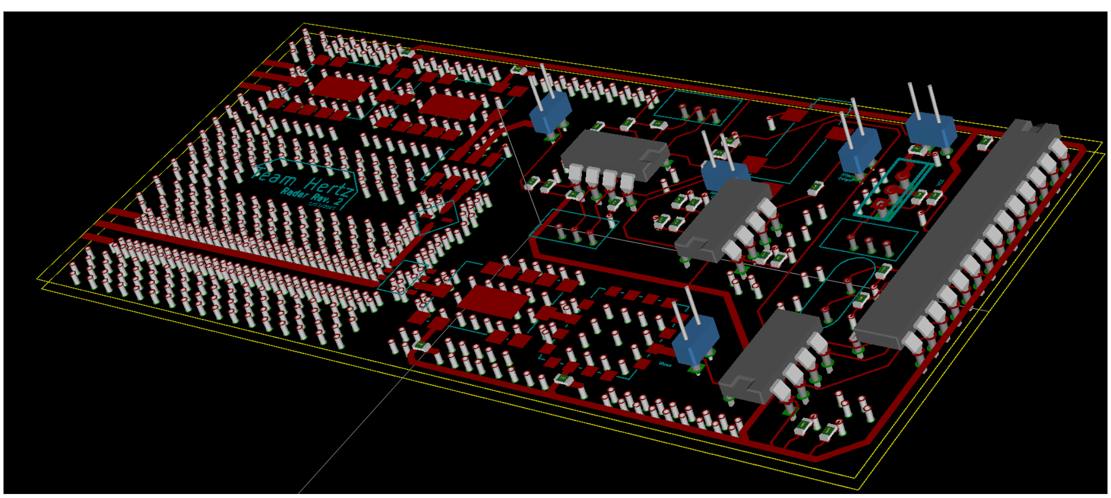

With the PCB layout completed, the Gerber files were generated and can be seen below. The Gerber files were then sent to Bay Area Circuits for manufacturing.

Gerber Output for Final PCB Layout

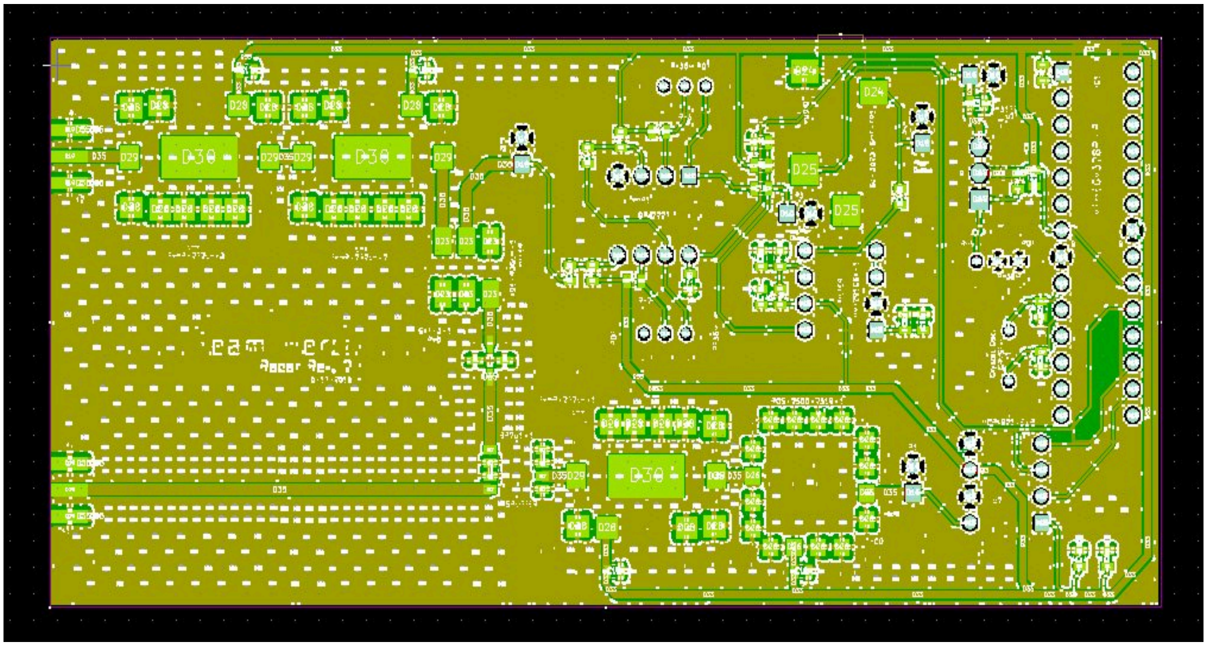

Patch Antenna Implementation

After performing the required analyses and determining the dimensions required to produce our desired response our patch antenna took shape. The patch antenna requires a probe feed which we modeled using a series of concentric cylinders as is shown in the bottom view:

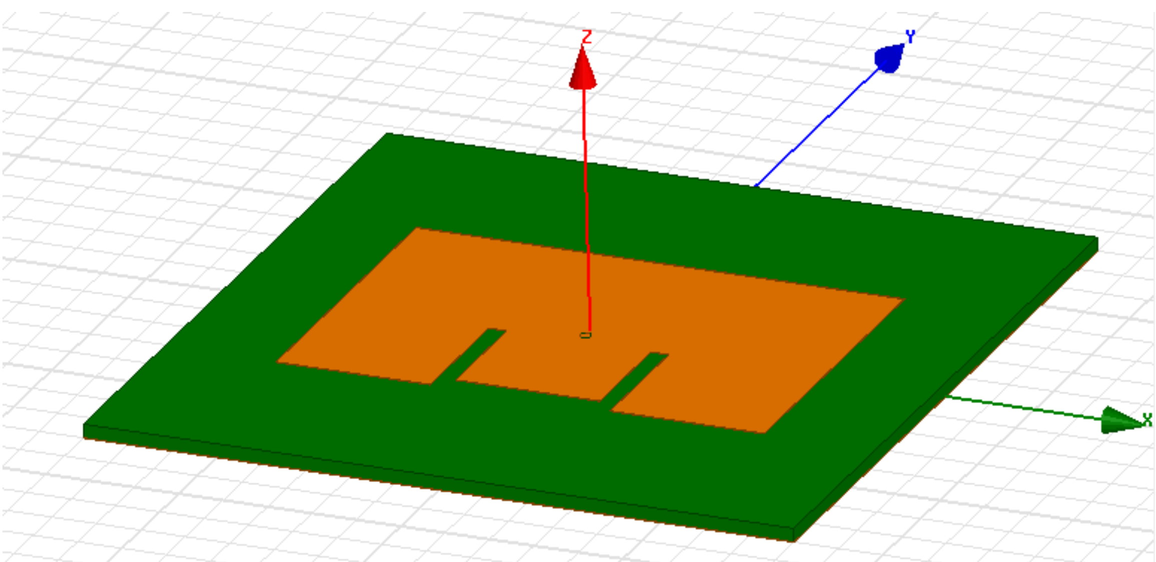

Bottom view:

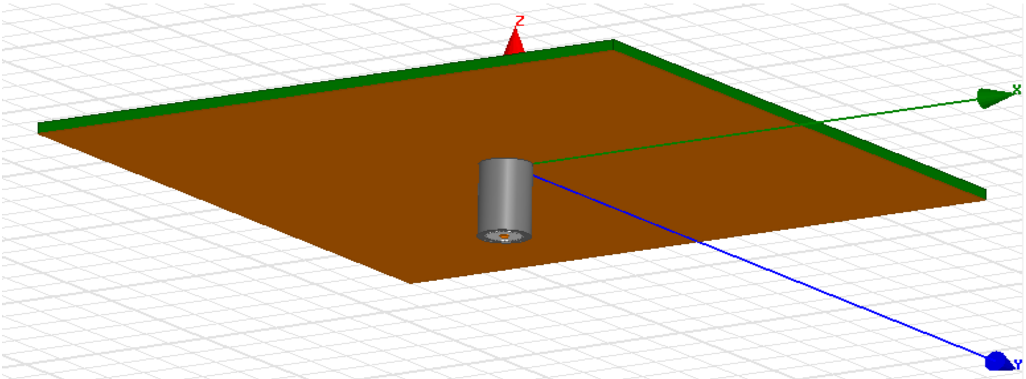

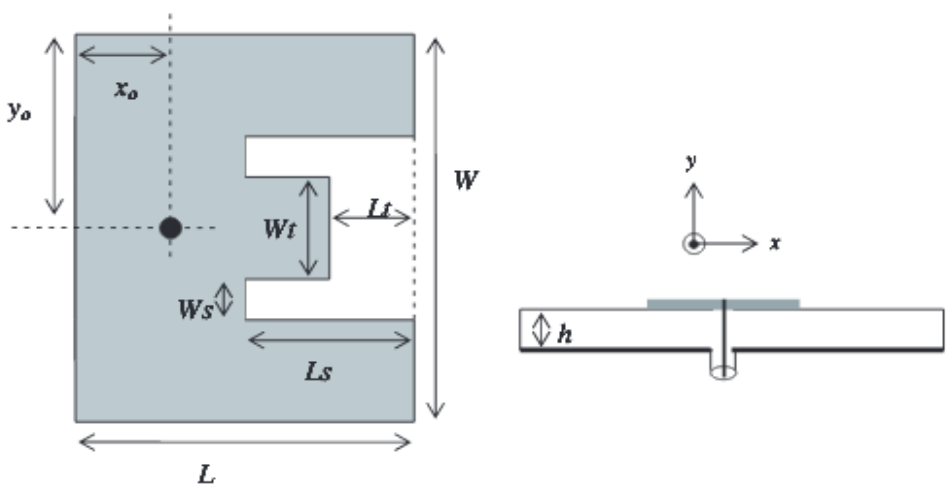

Dimension	Length (mm)
W	55
L	37
h	1.542
Ws	2
Lt	2
Wt	16.25
Xo	19.75
Yo	27.5
Ls	15.5

We ordered the Rogers RO4725JXR from the Rogers website and began fabrication as soon as we found a response we were satisfied with. Fabrication was done using this substrate and a milling machine to shape the copper of the patch, drill the hole for the probe, and finally to separate the patch from the rest of the unused material. We required SMA cables to connect our patch antennas to our RF board, so we used a cylindrical center conductor SMA jack in order to provide the probe feed. Before we soldered the jack in place we first scraped away some of the ground plane around the probe's intended location in order to make sure the center conductor does not contact the ground plane, and to make our finalized circuit perform more like our HFSS simulations. After this was done we soldered the body of the jack to the ground plane and soldered the center conductor to the patch on the other side. Our simulated patch antenna gave the following response:

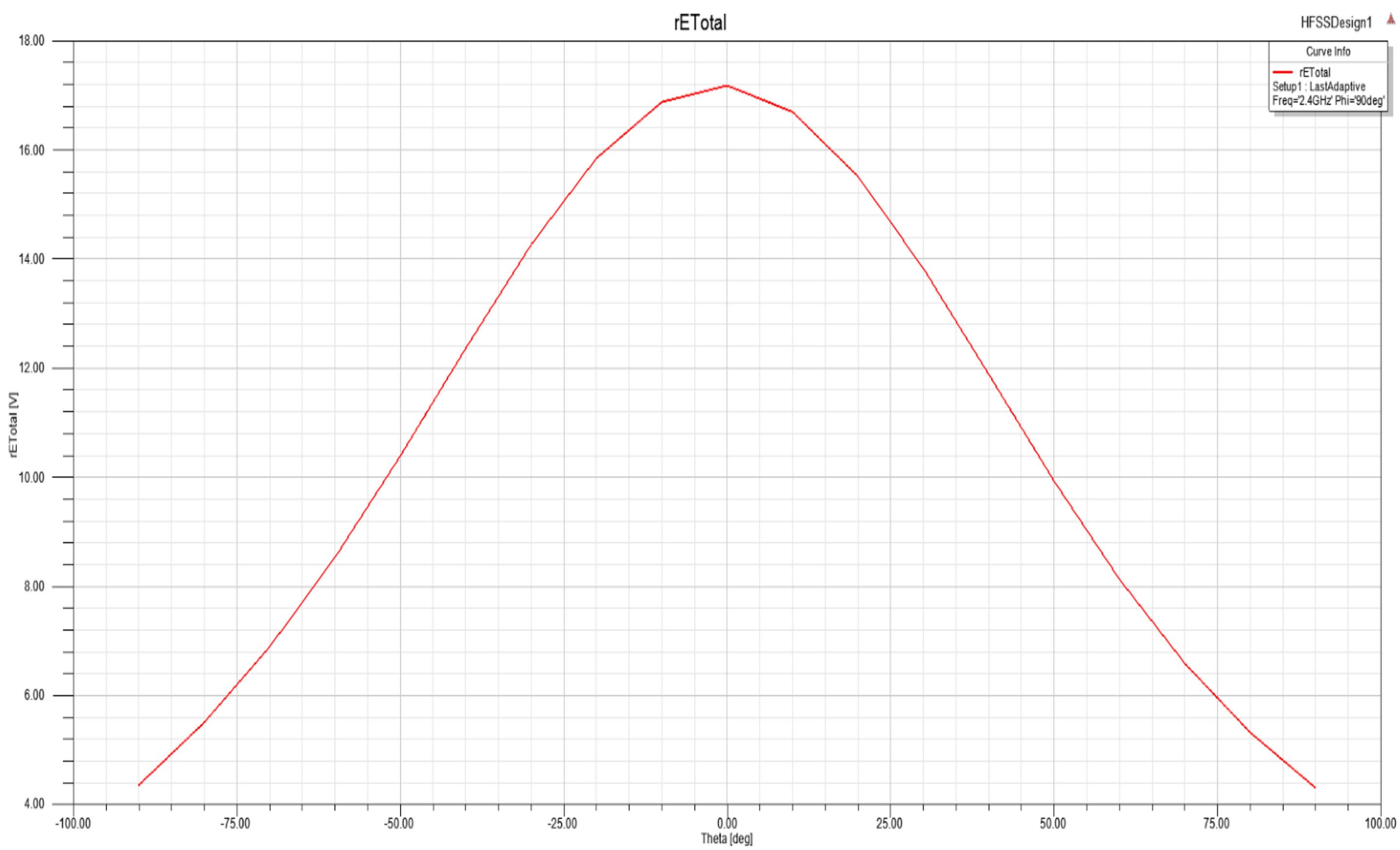

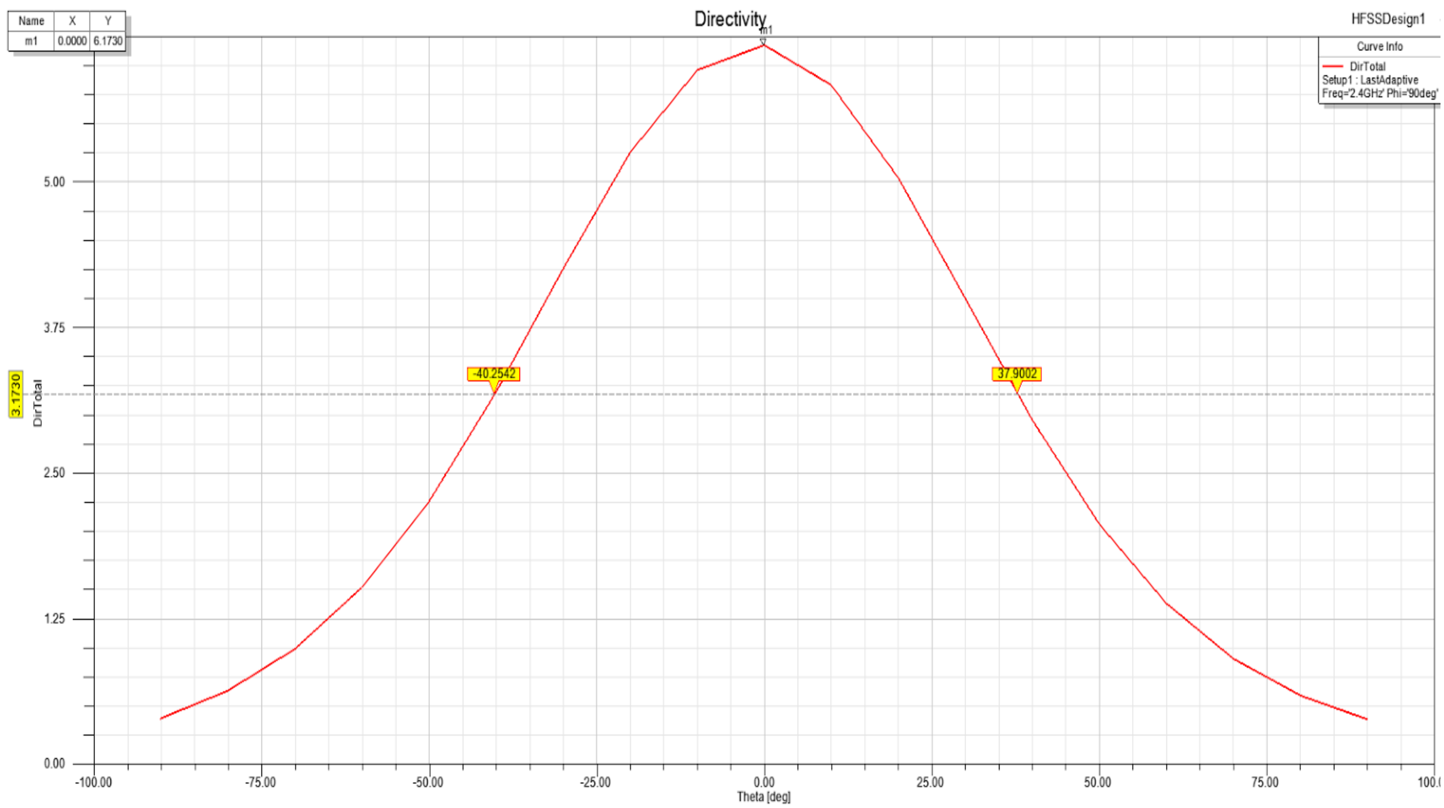

Directivity
HFSSDesign1
Name X Y
m1 0.0000 6.1730
Curve Info
DirTotal
Setup1 : LastAdaptive
Freq='2.4GHz' Phi='90deg'
-40.2542
37.9002
3.1730
DirTotal
Theta [deg]

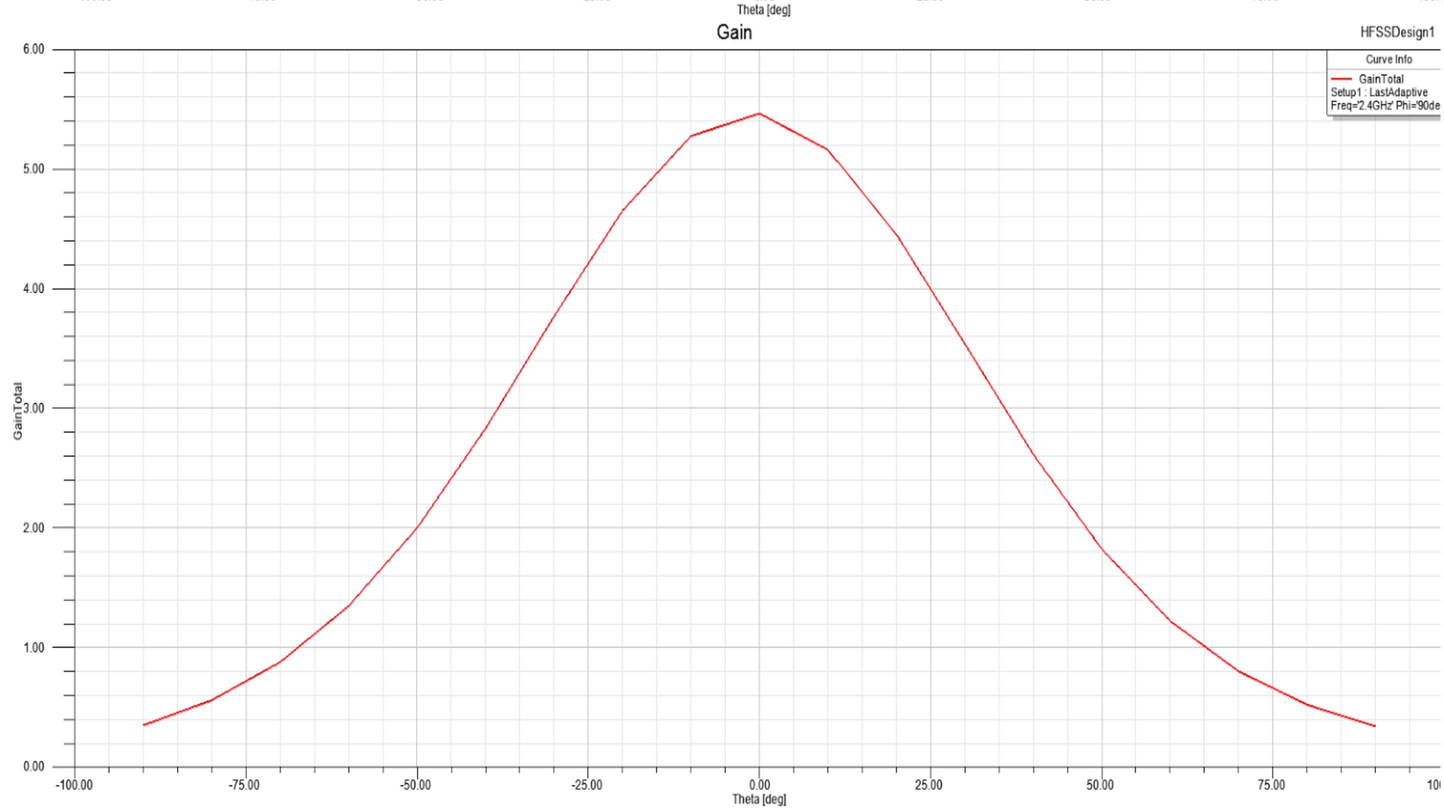

Gain
HFSSDesign1
Curve Info
GainTotal
Setup1 : LastAdaptive
GainTotal
Theta [deg]

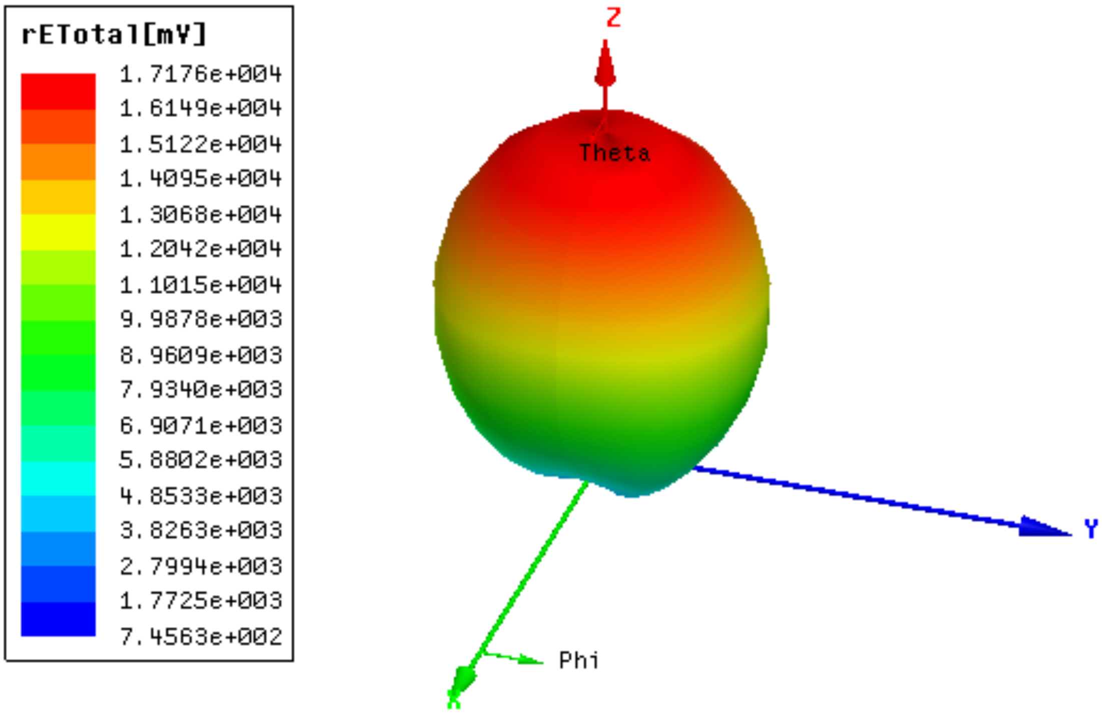
rETotal[mV]
1.7176e+004
1.6149e+004
1.5122e+004
1.4095e+004
1.3068e+004
1.2042e+004
1.1015e+004
9.9878e+003
8.9609e+003
7.9340e+003
6.9071e+003
5.8802e+003
4.8533e+003
3.8263e+003
2.7994e+003
1.7725e+003
7.4563e+002
Z
Theta
Y
Phi

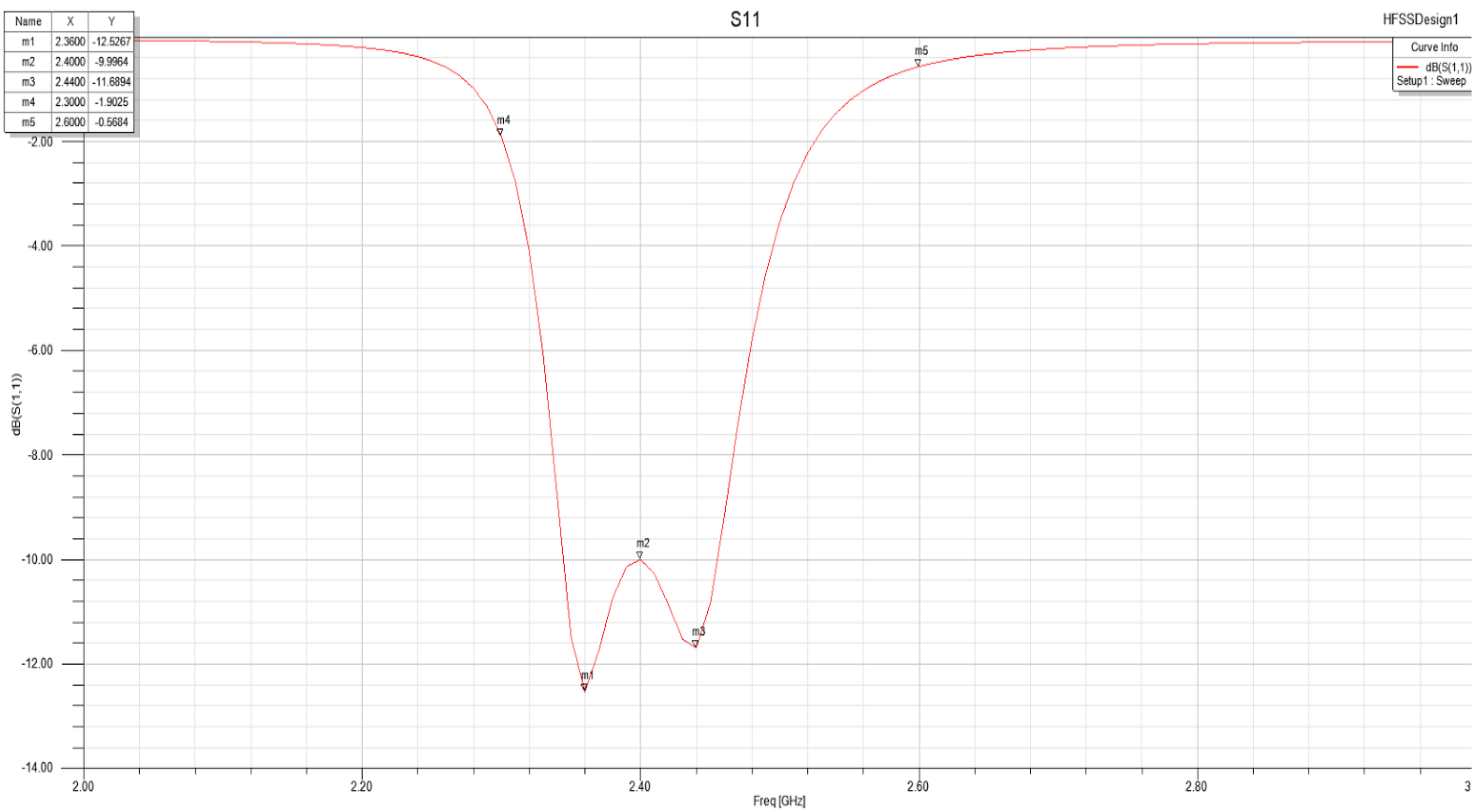
S11
HFSSDesign1
Name X Y
m1 2.3600 -12.5267
m2 2.4000 -9.9964
m3 2.4400 -11.6894
m4 2.3000 -1.9025
m5 2.6000 -0.5684
Curve Info
dB(S(1,1))
Setup1 : Sweep
dB(S(1,1))
Freq [GHz]
-2.00
-4.00
-6.00
-8.00
-10.00
-12.00
-14.00
2.00
2.20
2.40
2.60
2.80
3
m1
m2
m3
m4
m5

Testing and Performance

Radar Assembly

The radar consists of two parts that need to be assembled together: the PCB and the antennas. The assembly of the PCB took a while because we needed to solder on many components such as surface mount passives and ICs, through-hole ICs, and testing pins. On our first version of the PCB, there were a couple of 0402 components and very small ICs to solder with solder paste and a hot plate. That took a very long time since the footprints were too small to see with the naked eye, which led to the use of a microscope. Once the passives were all soldered on, we had to solder on the LNAs, which required the use of a microscope. It took us a couple of tries to solder on all four LNAs. We then soldered on the rest of the surface mount and through-hole components.

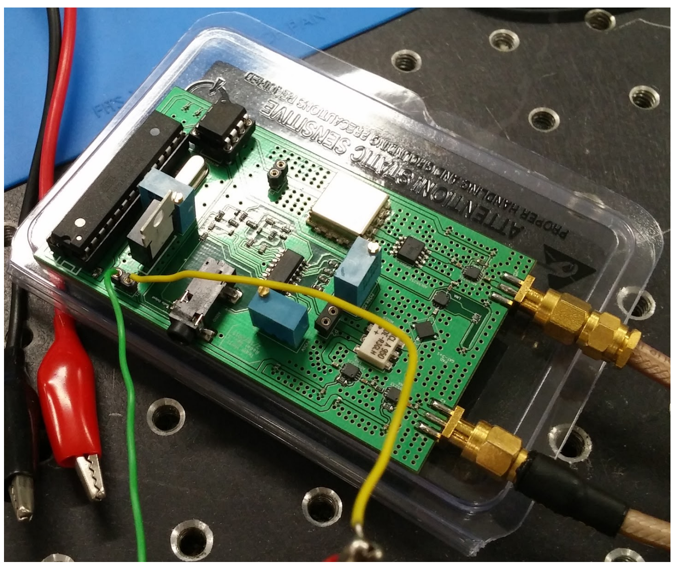

On our second version, we decided to use bigger modular ICs and 0603 components, so that it would be easier to see the footprints under the microscope and it would be easier to test. We then completed a similar assembly procedure as outlined for the pervious design. Using soldering paste and the hot plate, we soldered on the surface mount components and later soldered on the through-hole components. After that, we soldered on the SMA connectors that would be used to attach the antennas to the PCBs.

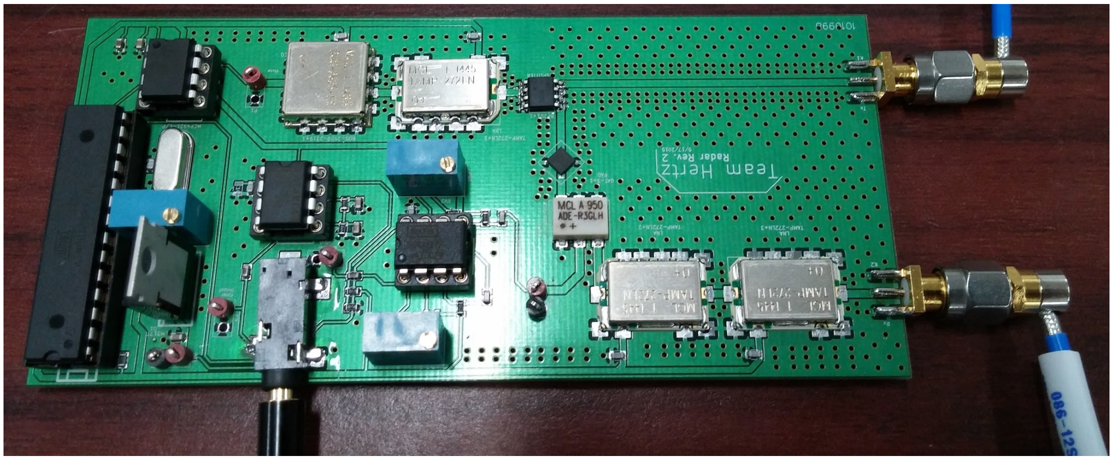

The antennas were to be attached to the PCB using SMA cables. We soldered on the flat part of the SMA connector to the ground plane of the antenna with the center pin soldered to the top copper layer.

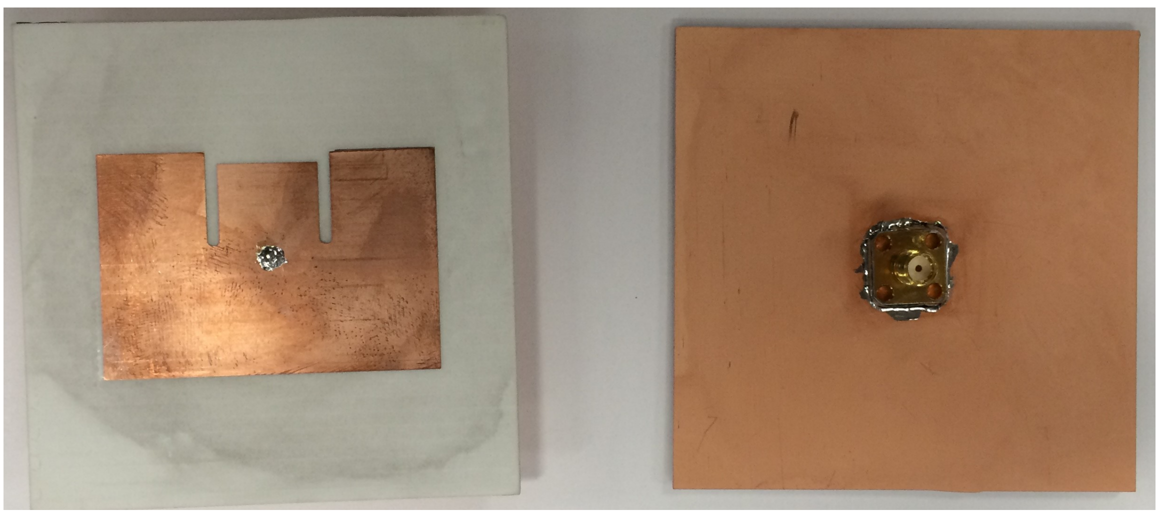

This is the final assembled radar system:

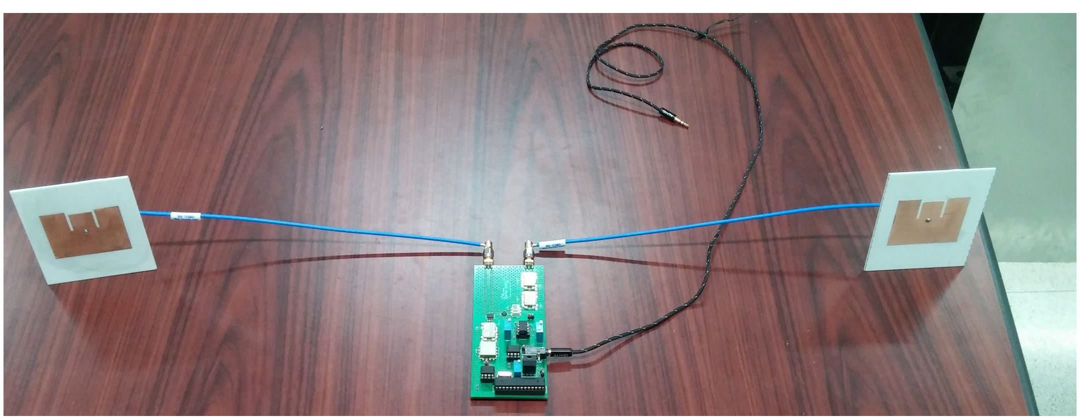

RF Subsystem Testing

The RF Subsystem was tested at two critical points. These points included the output of the transmit path and the IF output of the Mixer. By testing these two areas we were able to determine that the RF Subsystem was transmitting and receiving signals properly.

When testing the output of the transmit path the tuning voltage of the VCO was set to 2.15V which corresponds to 2.45 GHz. Theoretically, at 2.45GHz the system should be outputting around 15 dBm of power. When measuring the output of the system on the spectrum analyzer the response was as follows,

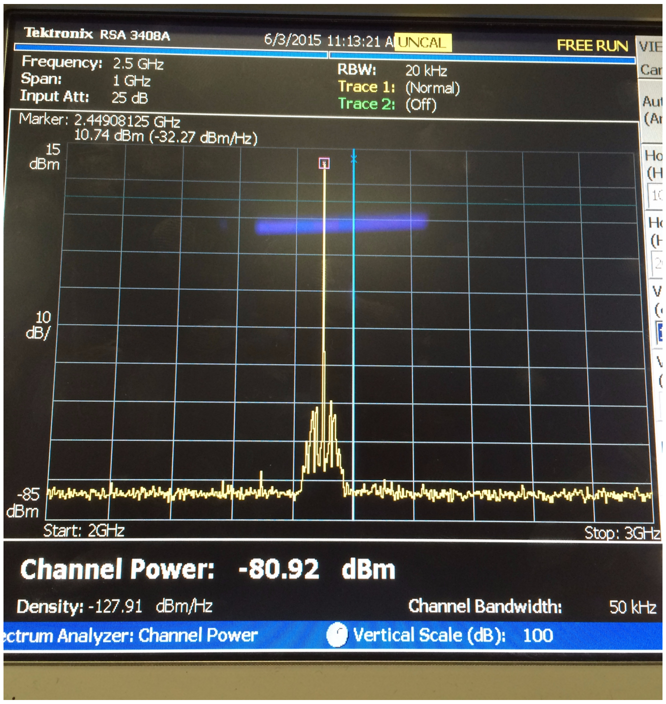

The spectrum analyzer indicates that the output power at the fundamental frequency is 10.74dBm. Nevertheless the coaxial cable that was utilized introduced a loss of approximately 4dB. Therefore, the true output power of the system came out to be 14.74dBm, which is very close to the expected value of 15dBm.
In order to test that the mixer was functioning correctly, the VCO output was set to 2.37GHz. Then, a signal generator was utilized to input a -13dBm signal at 2.371GHz into the receive end of the radar. As a result, when connecting the IF output of the mixer to an oscilloscope we'd expect a 1 MHz sinusoidal signal. The observed IF output is shown in the figure below.

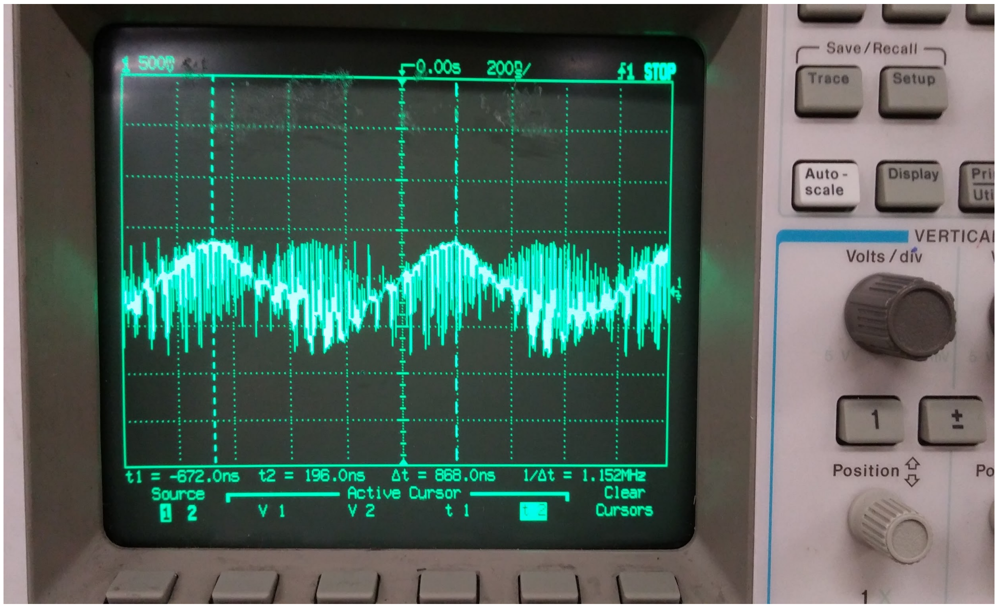

The figure above indicates that the IF output is at approximately 1 MHz. The noise that's observed on the signal was associated to parasitic effects caused by the oscilloscope itself as well as the mixer. Nevertheless, the baseband subsystem would certainly smooth the overall response.

In summary, the RF subsystem functioned properly at the two critical junctions. The transmit signal was at the power level that we designed for, and the mixer functioned properly.

Baseband Subsystem Testing

The testing of the baseband subsystem was initiated by first setting the tuning voltage Vtune of the modulator circuit to between 1 V and 3.75 V. This would ensure that the output of the VCO would have a frequency ranging from 2.3 GHz – 2.6 GHz. The output of the modulator circuit on the oscilloscope is shown below.

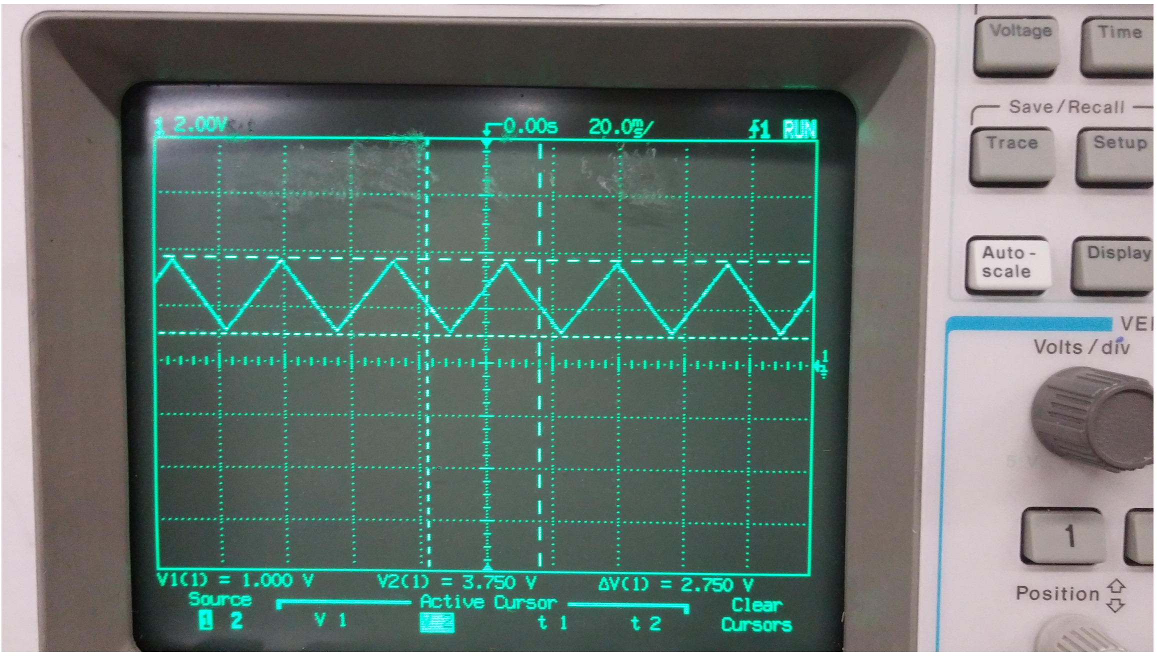

After it was determined that the modulator circuit was successfully working and the required tuning voltages were being obtained, we proceeded to test the gain stage individually by itself. The procedure to do this was to inject a 1 kHz signal (frequency chosen arbitrarily) with a 100 mVpp amplitude and tune the potentiometers on the gain stage until a 1 Vpp output was obtained from the gain stage. The output of the function generator was checked first to make sure that it was clean.

The picture below shows that the gain stage was successfully able to amplify a signal with amplitude 100 mVpp, resulting in a signal with amplitude approximately 1 Vpp.

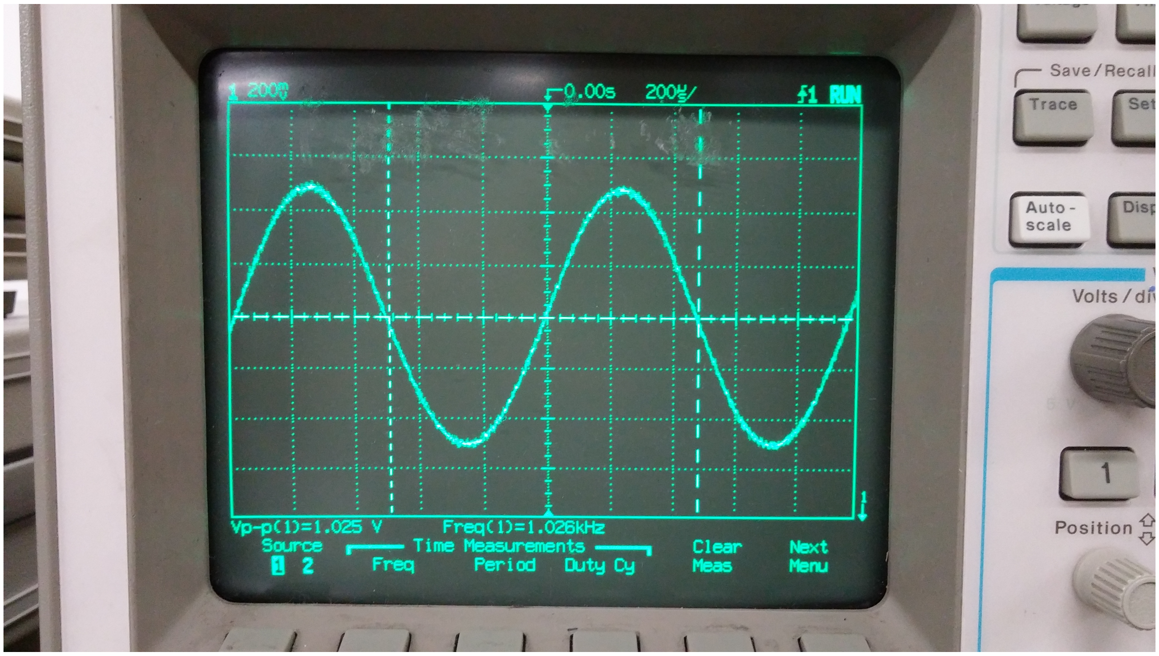

To test whether the gain stage would work for another frequency that was much higher (and would also be out of the passband of the LPF) we injected a 20 kHz signal with amplitude 100 mVpp. The picture below shows that the gain stage was indeed able to amplify this 20 kHz signal to give a signal with an amplitude of 1 Vpp.

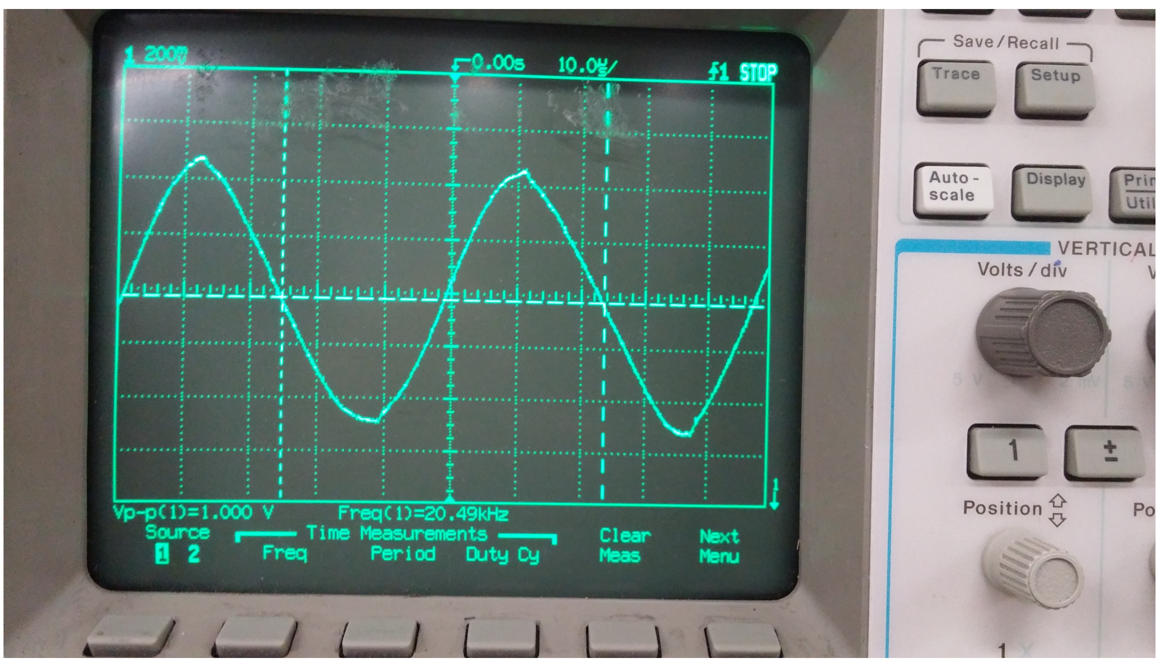

Therefore from the observations above we can conclude that the gain stage is successfully working.

The next step of the baseband subsystem testing was to check the true cutoff frequency of the LPF. To do this, a 1 kHz signal was injected directly into the input of the LPF, and the frequency was increased until the signal was no longer present on the oscilloscope. Using this procedure we experimentally determined the cutoff frequency of the LPF to be approximately 12 kHz. The result is shown below.

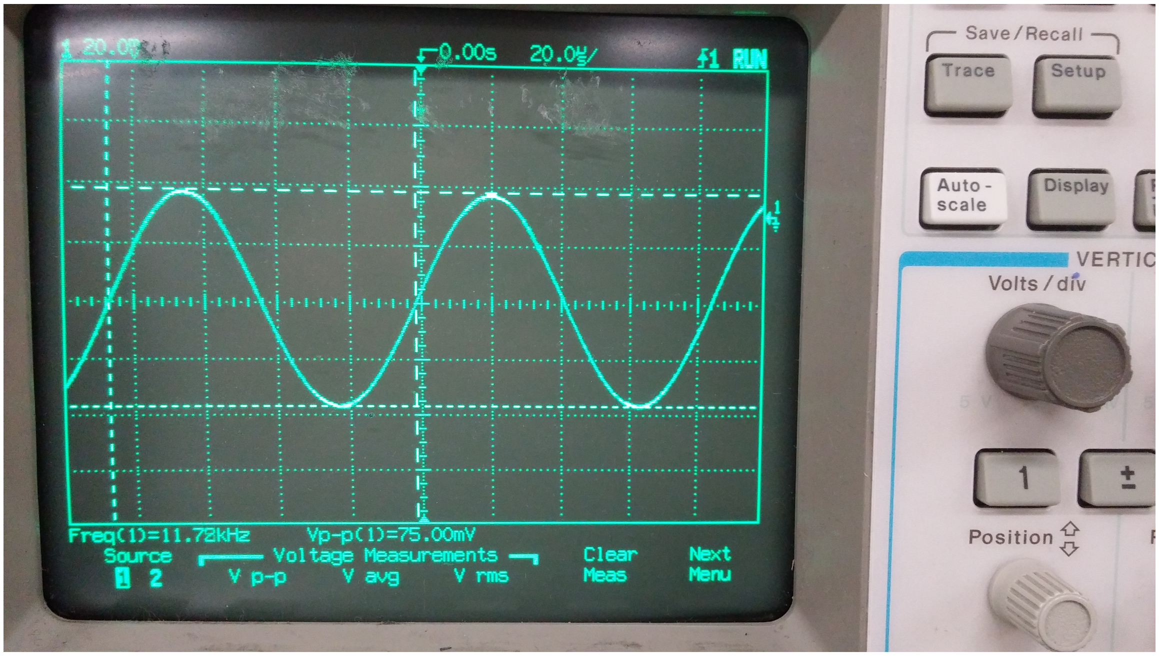

The test above had implicitly proved that the LPF would pass signals below 12 kHz since we were able to distinctly observe a signal at frequencies below this. Therefore the final thing to check was to see whether the LPF would totally reject frequencies far beyond the cutoff frequency. To test this, we injected a 20 kHz signal into the input of the LPF and checked the output. The picture below shows that the 20 kHz signal was totally attenuated and was not allowed to pass.

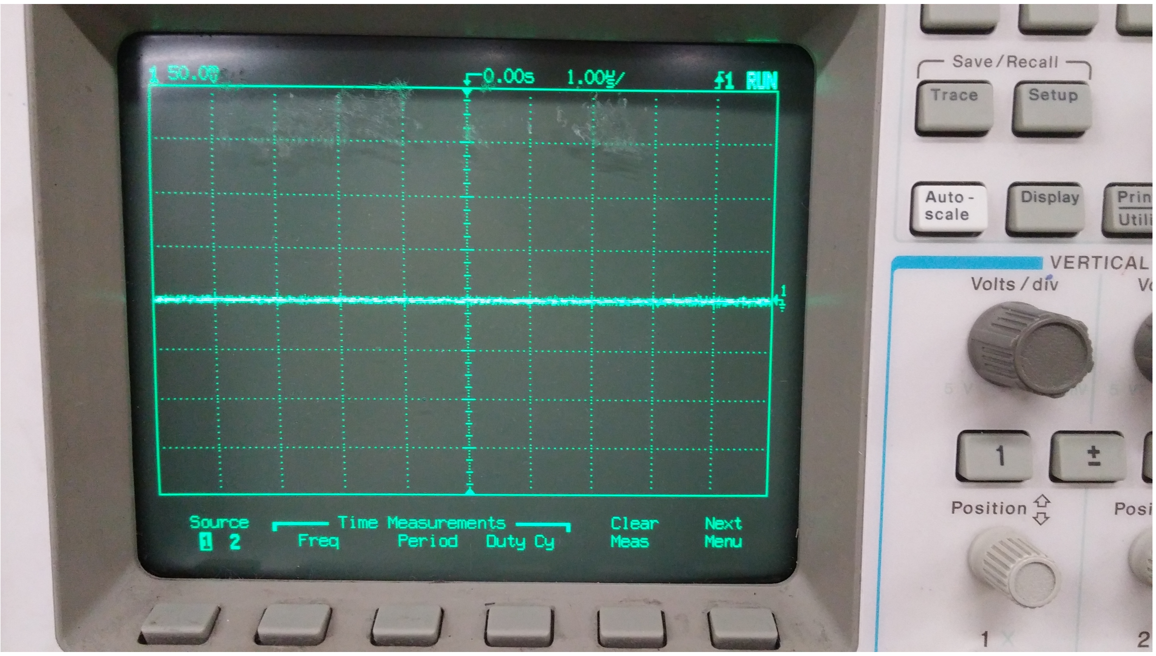

The results in the above pictures prove that the LPF stage is successfully working.

<u>Patch Antenna Testing</u>

Antenna testing took place in the anechoic chamber on the third floor of Kemper Hall. With some help from Christian Hurd we were able to test the antenna in a frequency range of 1.5 to 5.5 GHz and in a range of angles from -90° to 90°. Below are the S(2,1) values we received from a distance of roughly ten to eleven feet. The S(2,1) Vs. Frequency graph is where the antenna is set to 0° and the S(2,1) Vs. Angle graph is where the antenna is transmitting at our center frequency of 2.4 GHz. It looks as though our frequency response raised somewhat, likely due to errors in the milling process which caused a chunk of copper from the patch to come off. Overall the response falls about where we expected it to and the directivity is about what should be expected for a patch antenna of this design.

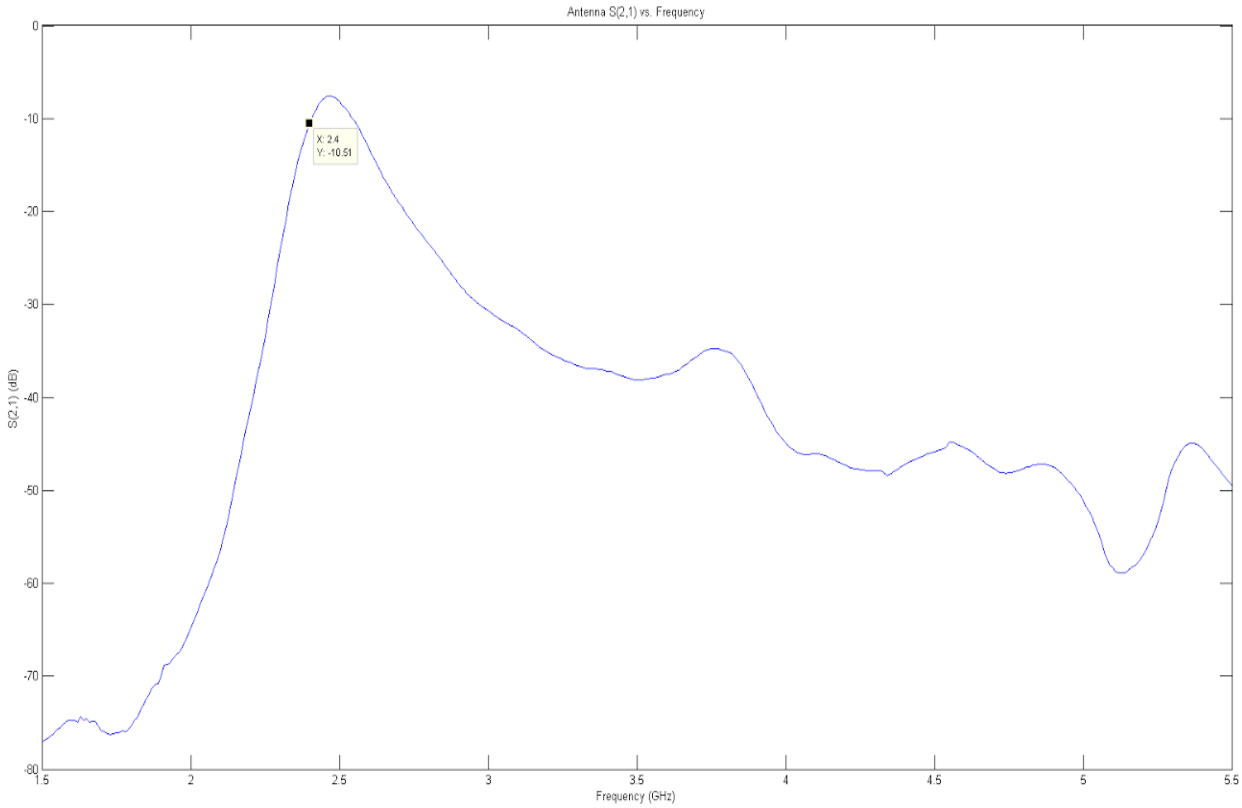
Antenna S(2,1) vs. Frequency
S(2,1) (dB)
Frequency (GHz)
X: 2.4
Y: -10.51
0
-10
-20
-30
-40
-50
-60
-70
-80
1.5
2
2.5
3
3.5
4
4.5
5
5.5

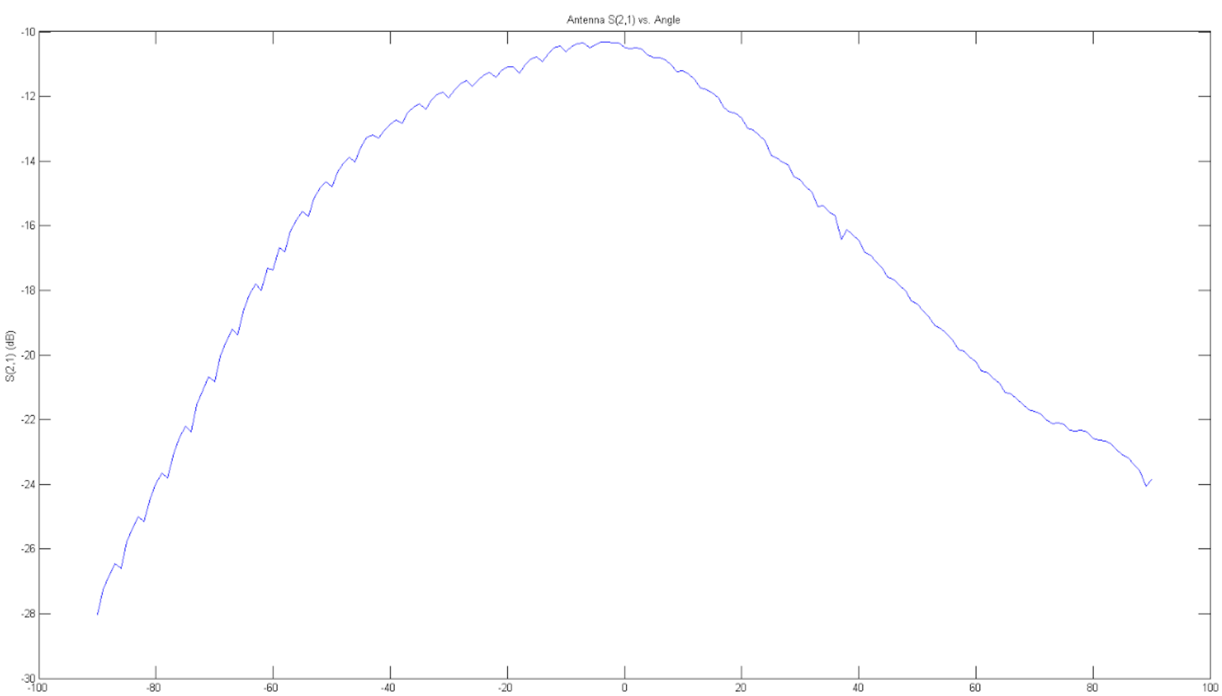
Antenna S(2,1) vs. Angle
S(2,1) (dB)
Angle (degrees)
-10
-12
-14
-16
-18
-20
-22
-24
-26
-28
-30
-100
-80
-60
-40
-20
0
20
40
60
80
100

Overall System Performance

Due to our earlier tests for each subsystem we conclusively proved that the individual subsystems of our entire circuit are working. Therefore we did not find any reason to doubt that any particular subsystem would fail. Another piece of evidence that strongly supported the above statements was the fact that the current draw of the circuit was exactly what it was predicted to be based on our current draw calculations. This was proven by reading the current drawn from the benchtop power supply. The picture of this is shown below.

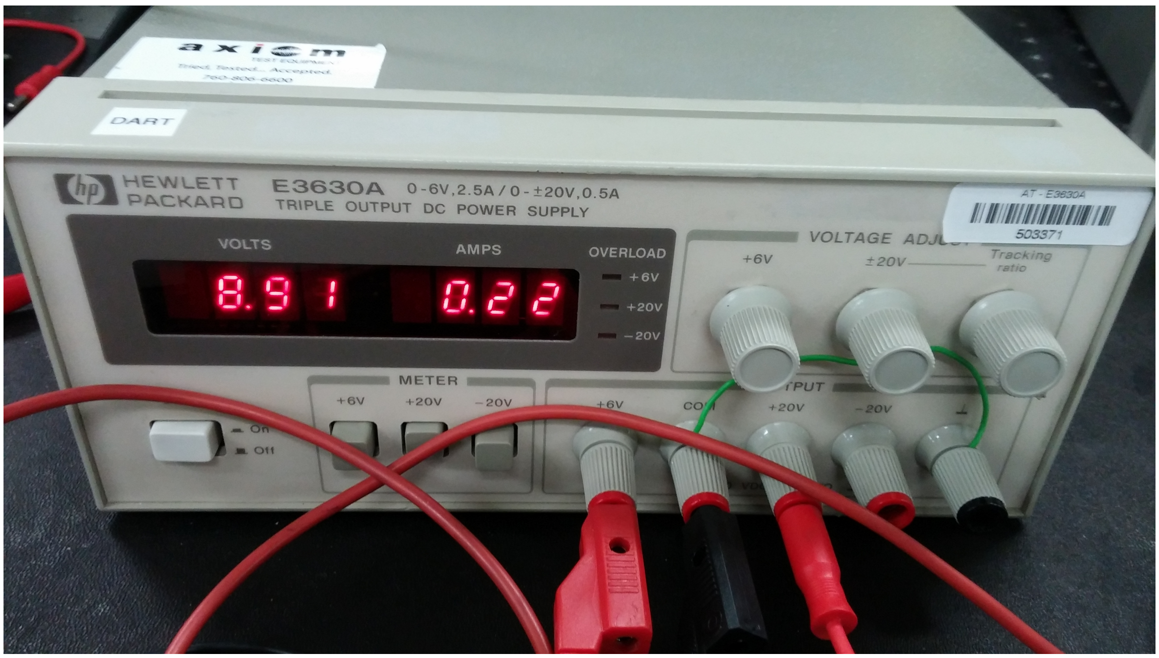

From the picture above it is readily seen that the overall current draw is about 220 mA, which is almost exactly what was predicted based on the current draw calculations in the RF subsystem section and the baseband subsystem section.

The final step to determine the overall system performance was to check whether the system could successfully detect a metal object. Thus, the overall system performance could be analyzed by looking at the results of the DSP code. To check if the radar was actually working we decided to perform the Doppler test first. The metal plate was placed about 1 m away from the antennas of the radar and slowly moved back and forth. The circuit was set to output a signal at only one frequency and then the real-time Doppler code was executed. The figures below show the output of this code.

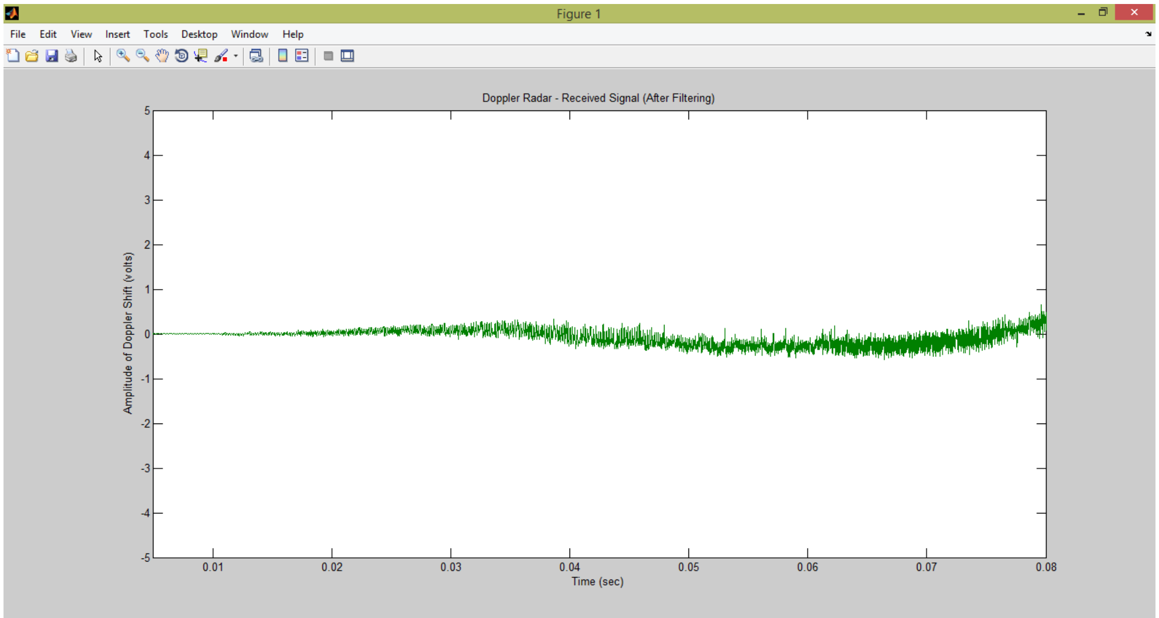
Figure 1
File Edit View Insert Tools Desktop Window Help
Doppler Radar - Received Signal (After Filtering)
Amplitude of Doppler Shift (volts)
Time (sec)

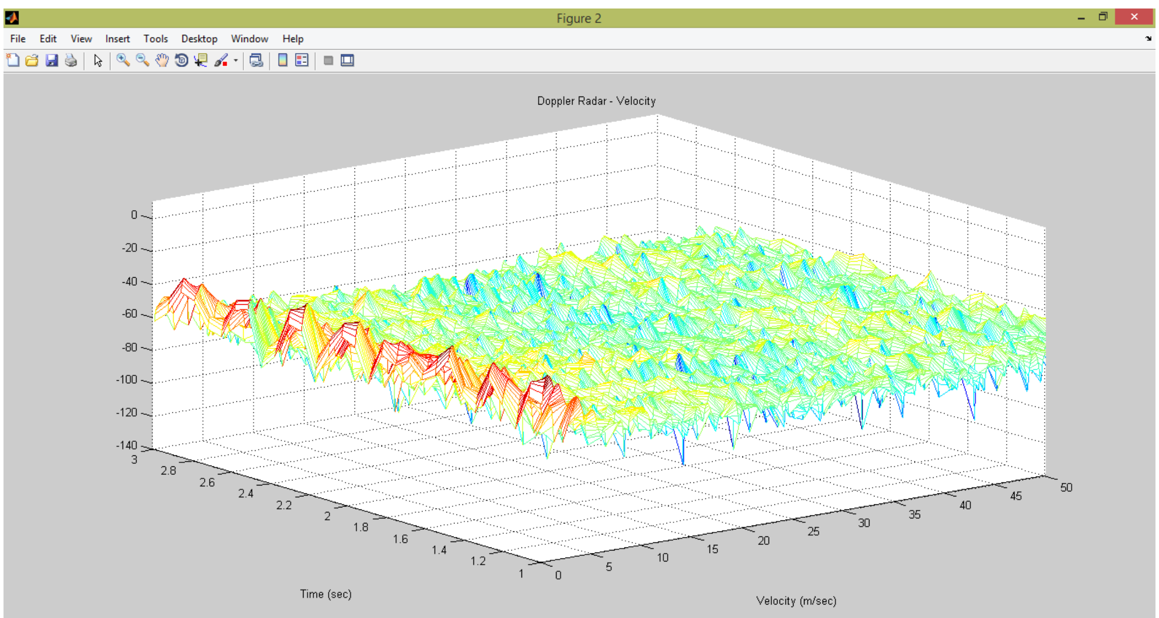
Figure 2
File Edit View Insert Tools Desktop Window Help
Doppler Radar - Velocity
Time (sec)
Velocity (m/sec)

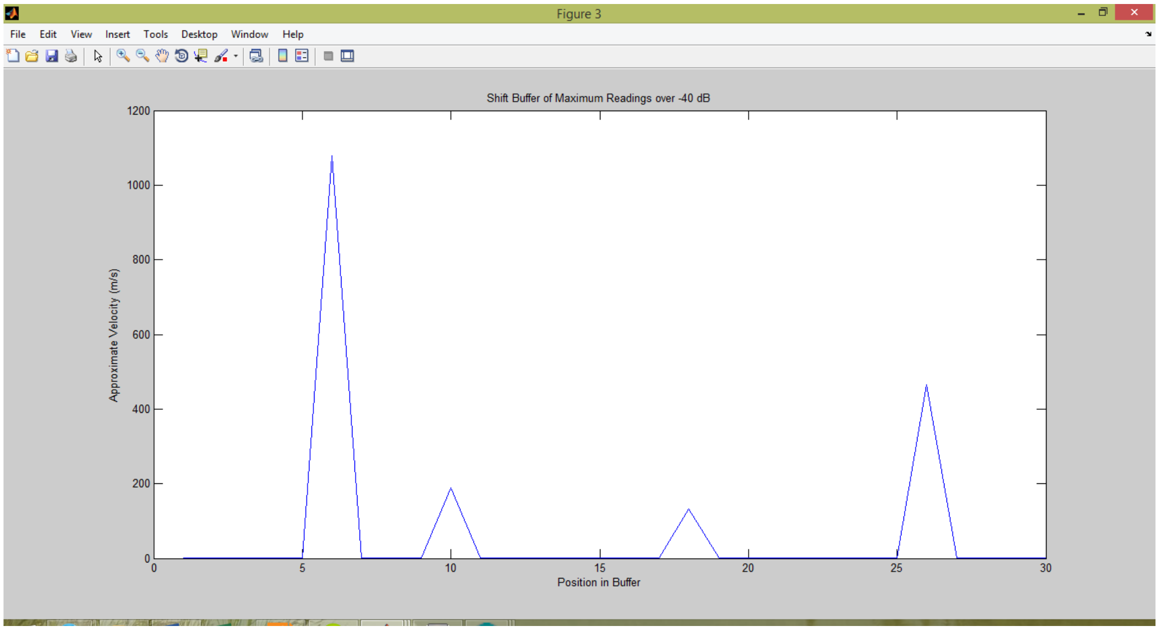

From the first plot we can see that the frequency of the IF signal is about 0.7 Hz. We can see this due to the fact that the signal shown lies between 0 Hz and 1 Hz. When doing our measurements we saw that the IF signal frequency fluctuated between 0 Hz and 1 Hz but for the most part was around 0.7 Hz. This is in complete agreement with the previous baseband IF frequency calculations for the Doppler test. Furthermore the Doppler test also proves that our overall system is able to successfully detect objects.

The next step to determine overall system performance was to check whether the radar would detect a stationary object. To this end a metal plate was placed 3 m away from the antennas of the radar. The radar was set to vary the frequency of the transmit signal and a .wav file was recorded using Audacity. This .wav file was later processed using MATLAB. The results are shown below.

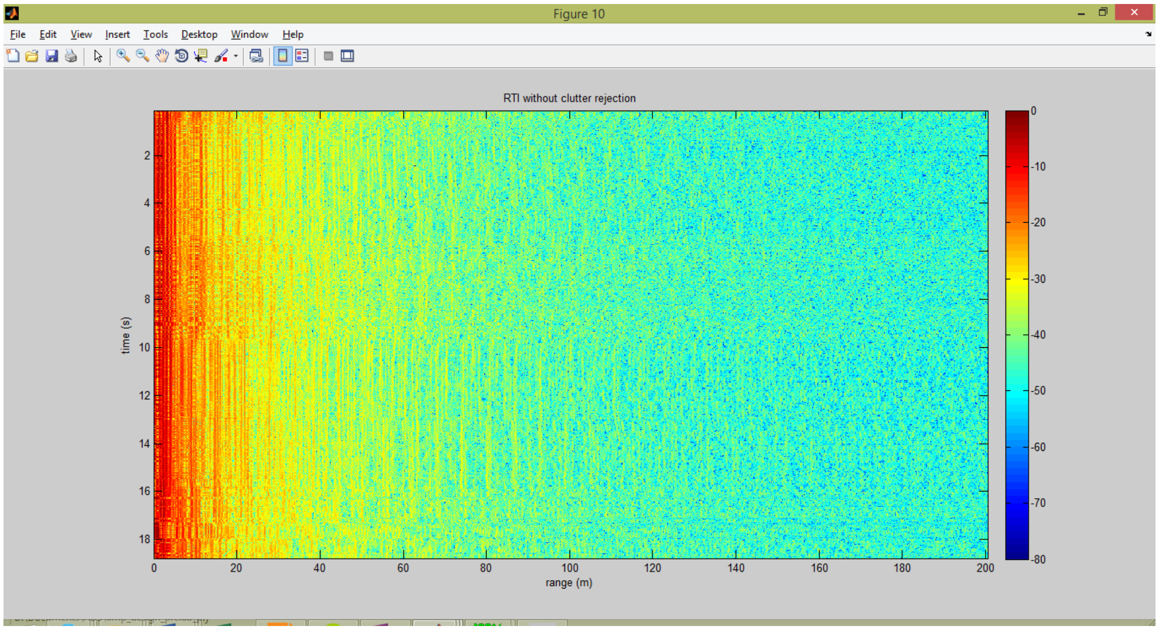

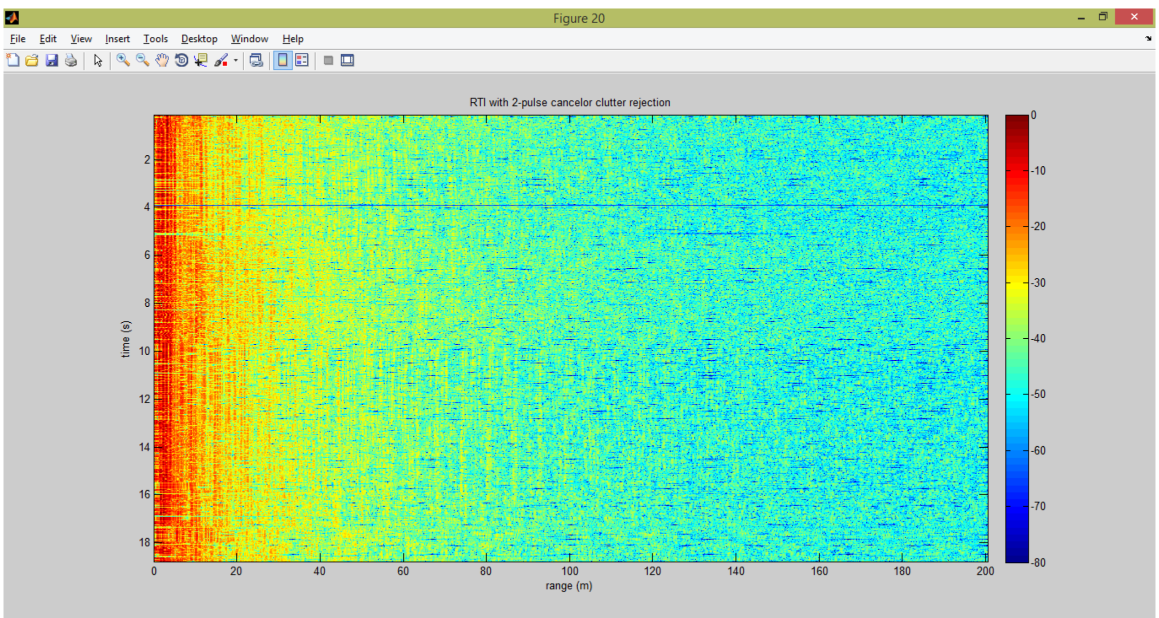

From the second plot above (which is the output using clutter rejection) we can see that the determined range is centered around 4-5 m since the red of the colormap is concentrated near 4-5 m. This agrees very well with the fact that the actual distance from the radar to the metal target was 3 m. Therefore we can conclude that the radar was able to detect a stationary object with reasonable accuracy.

Based on the successful evaluation of each individual subsystem, the low discrepancy between the actual vs. predicted current draw and reasonable performance in the two tests outlined in the competition guidelines we can conclude that the overall system performance is very acceptable.

Conclusion

The design and implementation of this system was meant to demonstrate and present a simple FMCW/Doppler radar that could be utilized in a wide range of applications. The RF and baseband subsystems presented the fundamental building blocks of a typical radar system, while the antenna outlined a unique design that would yield a wide bandwidth. In the design phase, the characteristics of the signals that would propagate throughout our system were specified. In the implementation and testing phase, we insured that the system was meeting these specifications. When tested individually, each of the fundamental blocks including the RF subsystem, baseband subsystem, and antenna were determined to be functioning properly. When testing the overall performance of the system it was determined that the system was properly measuring the velocity and position of a .3x.3m metallic target. Unfortunately due to the limited time we had, the system couldn't be fined tuned to insure precise Doppler and range measurements. Nevertheless, the system did function quite well as a whole and the critical design specifications were met. Overall, we were able to successfully present a footprint for designing and implementing a simple FMCW/Doppler radar with a wide variety of potential applications.

Individual Tasks and Contributions

Naveed Edalati

Designed the RF Subsystem, selected the RF components, completed the RF PCB Layout, assisted with the Baseband PCB Layout, tested the RF Subsystem, and worked on testing the overall system.

Rohan Phadke

Designed the Baseband Subsystem, selected the Baseband components, completed the Baseband PCB Layout, assisted with the RF PCB Layout, tested the Baseband Subsystem, worked on testing the overall system, and analyzed provided MatLab real-time Doppler and range code and interpreted results.

Charles Paulekas

Designed the Patch Antenna, assembled the PCB, purchased components, and maintained component inventory and finances.

Ruchika Jingar

Assisted with designing the Patch Antenna, assembling the PCB, and purchasing components.